(12)

RADC-TR-84-123
Interim Report
June 1984

A NEW LEAKY WAVE ANTENNA FOR MILLIMETER WAVES BASED ON THE GROOVE GUIDE

Polytechnic Institute of New York

P. Lampariello and A. A. Oliner

AD-A146 428

APPROVED FOR PUBLIC RELEASE; DISTRIBUTION UNLIMITED

DTIC FILE COPY

ROME AIR DEVELOPMENT CENTER
Air Force Systems Command
Griffiss Air Force Base, NY 13441

DTIC
ELECTE
OCT 0 1984
E

84 10 02 068

This report has been reviewed by the RADC Public Affairs Office (PA) and is releasable to the National Technical Information Service (NTIS). At NTIS it will be releasable to the general public, including foreign nations.

RADC-TR-84-123 has been reviewed and is approved for publication.

APPROVED: H. Steyskal

HANS STEYSKAL
Project Engineer

APPROVED:

FAUSTO E. MOLINET, Jr., Lt Colonel, USAF
Deputy Chief
Electromagnetic Sciences Division

FOR THE COMMANDER: John A. Ritz

JOHN A. RITZ
Acting Chief, Plans Office

If your address has changed or if you wish to be removed from the RADC mailing list, or if the addressee is no longer employed by your organization, please notify RADC EEAA) Hanscom AFB MA 01731. This will assist us in maintaining a current mailing list.

Do not return copies of this report unless contractual obligations or notices on a specific document requires that it be returned.

UNCLASSIFIED

SECURITY CLASSIFICATION OF THIS PAGE

REPORT DOCUMENTATION PAGE

1a. REPORT SECURITY CLASSIFICATION: UNCLASSIFIED	1b. RESTRICTIVE MARKINGS: N/A
2a. SECURITY CLASSIFICATION AUTHORITY: N/A	3. DISTRIBUTION/AVAILABILITY OF REPORT: Approved for public release; distribution unlimited.
2b. DECLASSIFICATION/DOWNGRADING SCHEDULE: N/A	
4. PERFORMING ORGANIZATION REPORT NUMBER(S): N/A	5. MONITORING ORGANIZATION REPORT NUMBER(S): RADC-TR-84-123
6a. NAME OF PERFORMING ORGANIZATION: Polytechnic Institute of New York; 6b. OFFICE SYMBOL (If applicable):	7a. NAME OF MONITORING ORGANIZATION: Rome Air Development Center (EEAA)
6c. ADDRESS (City, State and ZIP Code): 333 Jay Street, Brooklyn NY 11201	7b. ADDRESS (City, State and ZIP Code): Hanscom AFB MA 01731
8a. NAME OF FUNDING/SPONSORING ORGANIZATION: Rome Air Development Center; 8b. OFFICE SYMBOL (If applicable): EEAA	9. PROCUREMENT INSTRUMENT IDENTIFICATION NUMBER: F19628-81-K-0044
8c. ADDRESS (City, State and ZIP Code): Hanscom AFB MA 01731	10. SOURCE OF FUNDING NOS: PROGRAM ELEMENT NO 61102F; PROJECT NO 2305; TASK NO J3; WORK UNIT NO 30

11. TITLE (Include Security Classification): A NEW LEAKY WAVE ANTENNA FOR MILLIMETER WAVES BASED ON THE GROOVE GUIDE

12. PERSONAL AUTHOR(S):

13a. TYPE OF REPORT	13b. TIME COVERED	14. DATE OF REPORT (Yr., Mo., Day)	15. PAGE COUNT
Interim	FROM _____ TO _____	June 1984	58

16. SUPPLEMENTARY NOTATION: None

17. COSATI CODES			18. SUBJECT TERMS (Continue on reverse if necessary and identify by block number)
FIELD	GROUP	SUB. GR.	Millimeter waves; Groove guide; Antennas; Leaky wave antennas; Transverse equivalent network
09	05		

19. ABSTRACT (Continue on reverse if necessary and identify by block number)

Leaky wave antennas for millimeter waves face two main problems. The first relates to the small wavelengths involved, which require small waveguide dimensions and pose fabrication difficulties. The second problem is higher metal loss. In the new leaky wave antenna described and analyzed here, we overcome the first of these problems by choosing a structure with a longitudinally continuous aperture, and the second by basing the antenna on a low-loss waveguide, the groove guide.

The groove guide is an open waveguide, but its dominant mode is purely bound by virtue of structural symmetry. By placing a longitudinal asymmetric metal strip along the guide, the symmetry is disturbed and a new TEM-like mode is produced in the transverse direction that propagates to the open end and leaks

20. DISTRIBUTION/AVAILABILITY OF ABSTRACT	21. ABSTRACT SECURITY CLASSIFICATION	
UNCLASSIFIED/UNLIMITED ☐ SAME AS RPT. ☒ DTIC USERS ☐	UNCLASSIFIED	
22a. NAME OF RESPONSIBLE INDIVIDUAL: Hans Steyskal	22b. TELEPHONE NUMBER (Include Area Code): (617) 861-2052	22c. OFFICE SYMBOL: RADC (EEAA)

DD FORM 1473, 83 APR EDITION OF 1 JAN 73 IS OBSOLETE.

UNCLASSIFIED

SECURITY CLASSIFICATION OF THIS PAGE

power away.

An accurate theoretical analysis is presented for the performance properties of this antenna structure. The cross section is represented by a transverse equivalent network that contains some subtle features. All of the elements of this transverse network are obtained in closed form, so that the dispersion relation for the propagation characteristics is likewise in closed form.

Numerical values for the propagation characteristics are presented as a function of various geometric parameters. Design considerations, including an optimization procedure, are also described in some detail.

Accession For
NTIS CRA&I
DTIC TAB
Unannounced
Justification
By
Distribution/
Availability Codes
Dist | Avail and/or Special
A-1

DTIC COPY INSPECTED

TABLE OF CONTENTS

A. INTRODUCTION

Leaky wave antennas for the millimeter wave range face two main problems. The first relates to the small wavelengths involved, which require small waveguide dimensions and pose fabrication difficulties. The second problem is higher metal loss; for antennas which are many wavelengths long, the leakage (which results in radiation) may compete with the intrinsic waveguide loss, and the antenna design may be adversely affected. In this report, we present an analysis for a new type of leaky wave antenna for millimeter waves that addresses both of these problems. This new antenna overcomes the first of these problems by employing a longitudinally continuous aperture, and the second by basing the antenna on a low-loss waveguide, the groove guide.

The groove guide was one of several waveguiding structures proposed for millimeter wave use about 20 years ago in order to overcome the higher attenuation occurring at these higher frequencies. Although these new low-loss waveguides were introduced many years ago, they were not pursued beyond some initial basic studies because they were not yet needed. Now, millimeter waves are again becoming important, and attention is again being paid to new types of waveguides.

The open groove guide is shown in Fig. 1, and an indication of the dominant mode electric field lines present in its cross section is given in Fig. 2(a). One should first note that the structure resembles that of rectangular waveguide with most of its top and bottom walls removed. The groove guide can therefore be excited by providing a smooth tapered transition between it and a feed rectangular waveguide. Furthermore, if symmetry is maintained, many components can be designed for groove guide which are analogues of those in rectangular guide.

With respect to the low-loss nature of groove guide, we should recall that when the electric field is parallel to the metal walls the attenuation associated with those walls decreases as the frequency is increased; conversely, the attenuation increases with increasing frequency when the electric field is perpendicular to the walls. Since in groove guide the electric field is seen to be mostly parallel to the walls, its overall attenuation at higher frequencies is much lower than that of rectangular waveguide, where most of the field is perpendicular to the top and bottom walls.

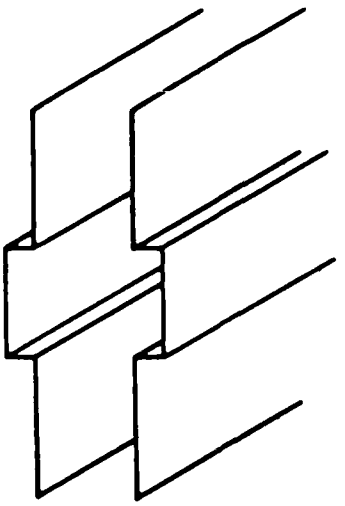

Fig. 1 The open groove guide, comprised of two parallel metal plates whose central regions are grooved outwards.

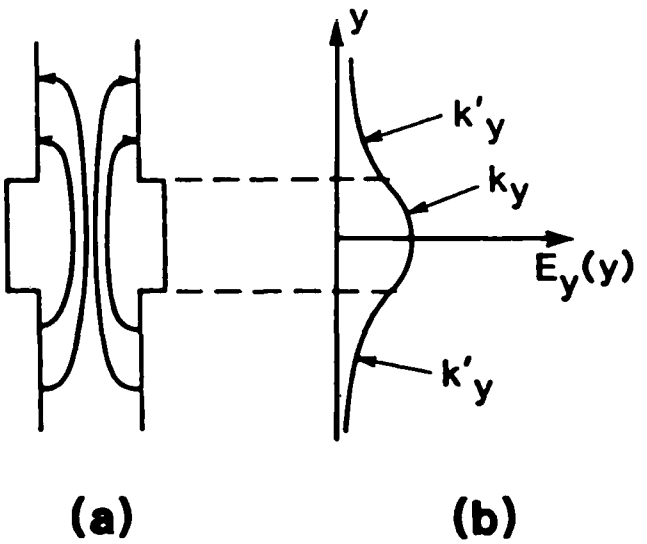

Fig. 2 The electric field of the dominant mode in open groove guide. (a) A sketch of the electric field lines in the cross section. (b) An approximate plot of the vertical component E_y as a function of vertical position y, showing that the guided mode is bound transversely to the central grooved region.

The greater width in the middle, or central, region was shown by T. Nakahara [1,2], the inventor of groove guide, to serve as the mechanism that confines the field in the vertical direction, much as the dielectric central region does in H guide. The field thus decays exponentially away from the central region in the narrower regions above and below, as shown in Fig. 2(b). If the narrower regions are sufficiently long, it does not matter if they remain open or are closed off at the ends.

Work on the groove guide progressed in Japan [2,3] and in the United States [4-6] until the middle 1960's, but then stopped and was later revived and developed further by D. J. Harris and his colleagues [7,8] in Wales. Their recent work is mainly experimental, being associated with components for groove guide. Other recent work includes that of J. Meissner, who investigated the coupling [9] between groove guides, and the radiation losses of bends [10]. To our knowledge, the present study represents the first contribution to antennas based on the groove guide.

A presentation of the new antenna structure and a brief summary of its properties were made recently in a pair of letters [11,12]. In this comprehensive report, we present a complete theoretical analysis together with numerical results and systematic design considerations.

The actual antenna structure and its operating principle are described in Section B. The basic principle is that of introducing asymmetry in the cross section so as to convert an initially bound mode into a leaky mode. Although it is applied here to a specific structure, this basic principle is quite general, and other asymmetry mechanisms can be employed to perform the same function, both in groove guide and in other open waveguides in which the basic mode is bound.

The properties of the leaky mode (which provides the radiating aperture for the antenna) are obtained from an accurate transverse equivalent network the constituents of which are derived in Section C. In these derivations it is necessary first to identify the correct transverse modes, and then to deduce expressions for the network constituents which are accurate but also simple in form, so that the resulting dispersion relation permits numerical calculations without undue complexity. We were fortunate in being able to derive all the network parameters in closed form. The most difficult constituent was that for the added asymmetric longitudinal strip that couples the leaking

transverse mode to the bound transverse mode. Its equivalent network is derived by employing small obstacle theory in a multimode context, where one of the modes is below cutoff, thereby requiring a modification in the expressions available in the literature.

From the complete transverse equivalent network, a dispersion relation is obtained which is in closed form. The dispersion equation and the numerical procedure employed to obtain specific numerical results are discussed in Section D.

In Section E we present design considerations for the leaky wave antenna together with a variety of numerical results. These design aspects include optimization considerations for the leakage constant, and the relations between the features of the radiation pattern and the phase and leakage constants. The antenna is seen to be capable of systematic design and to be versatile with respect to the scan angle and the beam width of the radiation.

B. THE OPERATING PRINCIPLE OF THE NEW ANTENNA

The new leaky wave antenna is shown in Fig. 3. The basic difference between the structures in Figs. 1 and 3 is that in Fig. 3 a continuous metal strip of narrow width has been added to the guide in asymmetrical fashion. Without this strip, the field of the basic mode of the symmetrical groove waveguide is evanescent vertically, so that the field has decayed to negligible values as it reaches the open upper end. The function of the asymmetrically placed metal strip is to produce some amount of net horizontal electric field, which in turn sets up a mode akin to a TEM mode between parallel plates. The field of that mode propagates all the way to the top of the waveguide, where it leaks away. It is now necessary to close up the bottom of the waveguide, as seen in Fig. 3, to prevent radiation from the bottom, and (nonelectrically) to hold the structure together. Of course, the upper walls could end as shown in Fig. 3 or they could attach to a ground plane.

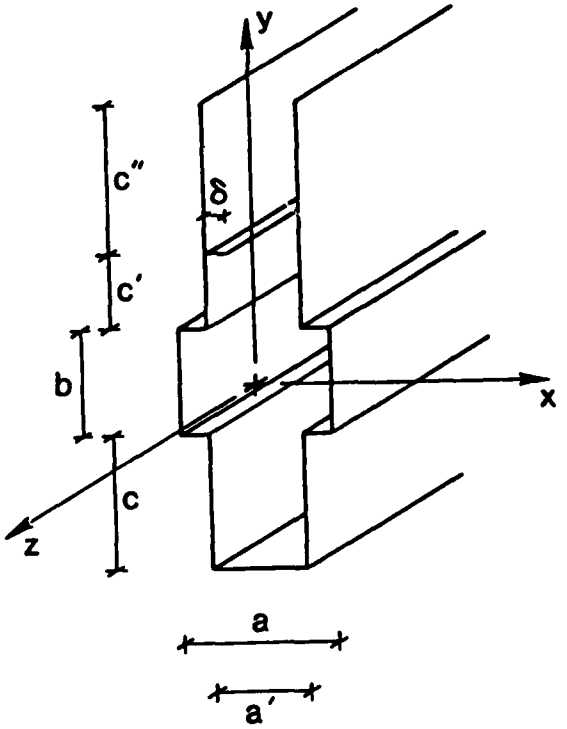

Fig. 3 Cross section of the new leaky wave antenna, where leakage is produced by the introduction of an asymmetric continuous metal strip of width δ.

The structure in Fig. 3 now yields a leaky wave line-source antenna of simple configuration, since it is longitudinally continuous. The value of the phase constant β of the leaky wave is governed primarily by the properties of the original unperturbed groove guide, and the value of the attenuation, or leakage, constant α is determined by the width and location of the perturbing strip. As discussed in Section E, standing waves associated with the added mode created by the asymmetry introduce additional problems in the design, but these problems can be overcome by certain optimization considerations.

As mentioned in the Introduction, the asymmetry can be produced in other ways, resulting in different actual structures but with antennas that perform similarly. This particular structure was chosen because it is amenable to accurate analysis in a simple way, as explained in detail in the next section.

C. THE TRANSVERSE EQUIVALENT NETWORK

The complete transverse equivalent network for the antenna structure depicted in Fig. 3 is derived below by viewing it as an open waveguide with a complex propagation wavenumber $\beta - j\alpha$ in the z direction. The dispersion relation for β and α is obtained in Section D by applying the transverse resonance condition to this transverse equivalent network.

In this transverse equivalent network, the uniform regions of the open waveguide's cross section are represented by transmission lines, and junctions or other discontinuities are represented by lumped elements. The first step in the derivation of the network is therefore the identification of the correct transverse modes which the transmission lines represent. The lumped elements must then be recognized or derived corresponding to the various discontinuities present in the cross section.

As discussed in Section B, the antenna is created by introducing into the basic nonradiating groove guide an additional longitudinally continuous metal strip. The strip is introduced in asymmetrical fashion so as to produce some net horizontal electric field. In effect, a new transverse mode is created thereby, which propagates (at an angle) all the way to the top of the waveguide, where it leaks away, thus transforming the initially bound longitudinal mode into a leaky one. The transverse equivalent network must therefore be based on these two transverse modes, which propagate in the y direction and are coupled together by the added strip. The coupled transverse modes then combine, of course, to produce a net TE longitudinal mode (in the z direction) with a complex propagation constant $\beta - j\alpha$.

The basic form of the transverse equivalent network is shown in Fig. 4, where the network has been placed on its side for clarity. In the network, the i=1 transmission lines represent the original mode (the dominant nonradiating mode) with a half sine variation in the x direction in Fig. 3, and the i=0 transmission lines represent the new mode which has no variation with x. The characteristic admittances Y and the transverse wavenumbers k_y of these transmission lines must be properly identified and related, and expressions for the lumped elements representing the various discontinuities in the cross section must be derived. The proper mode identifications and the mode functions corresponding to the transmission lines are discussed in the next

subsection. In subsequent subsections, expressions are presented or derived for the step junctions, the asymmetrical coupling strip, and the radiating open end. In the final subsection of Section C, the various constituents are combined to produce the complete transverse equivalent network.

1. The Transverse Modes

To properly characterize the transmission lines in the transverse equivalent network in Fig. 4, we must identify the correct modes in the y direction. We first note that with respect to the z (longitudinal) direction the overall guided mode is a TE (or H) mode; that is, there exists only a component of H in the z direction. This result is to be expected since the groove guide consists of a perfectly conducting outer structure filled with only a single dielectric material (air). In the y direction, however, there exist <u>both</u> E_y and H_y components, so that the mode is <u>hybrid</u> in that direction.

Since the groove guide is <u>uniform</u> in the z direction, and its field has only an H_z component, a hybrid mode in the y direction is seen to be what is called by some an H-type mode with respect to the z direction, and by others an LSE mode with respect to the z direction. We prefer the former notation, and we shall designate a hybrid mode in the y direction as an $H^{(z)}$-type mode . Altschuler and Goldstone [13] discuss such modes in detail and present the field components for them and the characteristic admittances for transmission lines representative of them.

For the transmission lines in Fig. 4 we therefore require the mode functions and transmission line properties of an $H^{(z)}$ -type mode in parallel-plate guide, which propagates in the y direction and is hybrid in that direction, but has only an H_z component in the z direction. The coordinate system we employ is that given in Fig. 3, but it differs by a rotation from the one employed in reference [13]. In our transverse equivalent network, we are concerned with two different $H^{(z)}$ -type modes in the y direction, the $i = 1$ and the $i = 0$ modes. We recognize that in the sum-of-squares relation

$$k^2 = k_x^2 + k_y^2 + k_z^2 \tag{1}$$

the longitudinal propagation wavenumber $k_z (= \beta - j\alpha)$ is the same for both modes, and the unknown k_y values are designated as k_{y1} and k_{y0}. The k_x

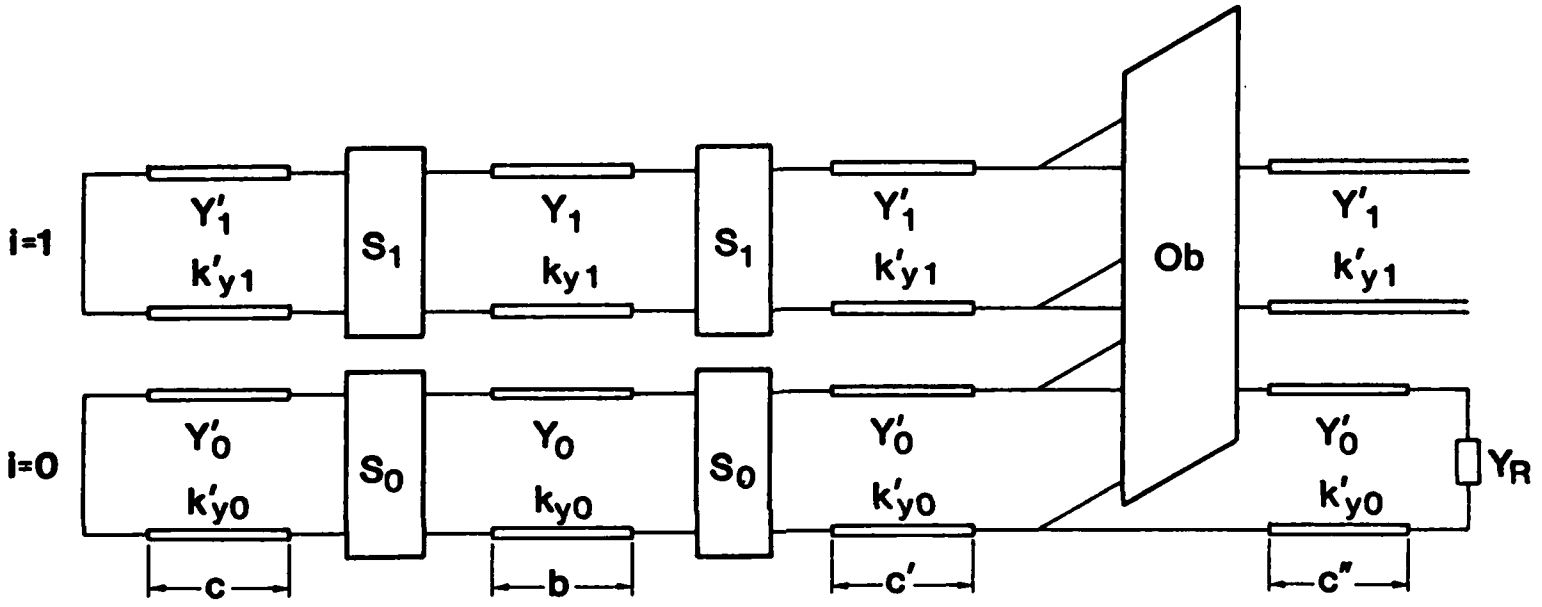

Fig. 4 Basic form of the transverse equivalent network that couples the exciting dominant transverse mode i = 1 and the radiating transverse mode i = 0, in accordance with the cross section shown in Fig. 3. The boxes labeled S and Y_R represent respectively the step junctions and the radiating open end, and the box labeled Ob signifies the coupling network corresponding to the perturbing asymmetric strip obstacle. (For clarity, the network is placed horizontally rather than vertically.)

values are $k_{x1} = \frac{\pi}{a}$ and $k_{x0} = 0$, consistent with their known variations with x. The characteristic admittance for either of the modes is given by [13] as

$$Y = \frac{k^2 - k_z^2}{\omega\mu k_y} = \frac{1}{Z} \tag{2}$$

where k_y is of course the propagation wavenumber of the transverse transmission line.

The components of the electric and magnetic fields (of these transverse modes) that are transverse to the y direction are given by the usual expressions

$$\underline{E}_t(x,y,z) = V(y)\underline{e}(x,z) \tag{3}$$

$$\underline{H}_t(x,y,z) = I(y)\underline{h}(x,z) \tag{4}$$

where the voltage V(y) and current I(y) satisfy the transmission line equations in the y direction, and $\underline{e}$ and $\underline{h}$ are mode functions dependent only on the cross section to y. Consistent with the specification (2) for characteristic admittance, the electric and magnetic field vector mode functions, $\underline{e}$ and $\underline{h}$, satisfy the orthonormality condition

$$\int_s \underline{h} \times \underline{y}_o \cdot \underline{e}^* \, dS = 1$$

where the integration is performed over the cross section normal to $\underline{y}$, and we have

$$e_x(x,z) = -h_z(x,z)$$

The z dependence everywhere is understood to be $\exp(-jk_z z)$.

For the parallel-plate region, using (5), we find for the i=1 mode

$$e_{x1}(x,z) = \sqrt{\frac{2}{a}} \sin\frac{\pi x}{a} e^{-jk_z z} = -h_{z1}(x,z) \tag{7}$$

We will need the h_{y1} component of the mode function in the derivation of the expression for the added coupling strip. That component is obtained from

$$h_y(x,z) = \frac{-jk_y}{k^2 - k_z^2} \frac{\partial h_z(x,z)}{\partial z}$$

yielding

$$h_{y1}(x,z) = \sqrt{\frac{2}{a}} \frac{k_{y1}k_z}{k^2-k_z^2} \sin \frac{\pi x}{a} e^{-jk_z z} \tag{8}$$

Correspondingly, for the i=0 mode, we have

$$e_{x0}(x,z) = \sqrt{\frac{1}{a}} e^{-jk_z z} = -h_{z0}(x,z) \tag{9}$$

$$h_{y0}(x,z) = \sqrt{\frac{1}{a}} \frac{k_{y0}k_z}{k^2-k_z^2} e^{-jk_z z}$$

or

$$h_{y0}(x,z) = \sqrt{\frac{1}{a}} \frac{k_z}{k_{y0}} e^{-jk_z z} \tag{10}$$

from $k^2 = k_{y0}^2 + k_z^2$, since $k_{x0} = 0$. The fields simplify considerably for the i=0 mode. As seen, the mode functions do not depend on x, and the mode is in fact not hybrid but a TE mode in the y direction, having E_x, H_y and H_z components only. As a result, expression (2) for the characteristic admittance reduces to

$$Y_0 = \frac{k_{y0}}{\omega\mu} = 1/Z_o \tag{11}$$

The following complete summary of the field components for the i=1 and i=0 modes is obtained on use of (3) and (4) together with the mode functions above and the remaining ones obtained in the same fashion;

$$E_x(x,y,z) = \left[V_0(y) \sqrt{\frac{1}{a}} + V_1(y) \sqrt{\frac{2}{a}} \sin \frac{\pi}{a} x \right] e^{-jk_z z}$$

$$E_y(x,y,z) = -jI_1(y) \sqrt{\frac{\mu}{\varepsilon}} \frac{k}{k^2-k_z^2} \sqrt{\frac{2}{a}} \frac{\pi}{a} \cos \frac{\pi}{a} x \, e^{-jk_z z}$$

$$E_z(x,y,z) = 0$$

$$H_x(x,y,z) = jI_1(y) \frac{k_z}{k^2-k_z^2} \sqrt{\frac{2}{a}} \frac{\pi}{a} \cos \frac{\pi}{a} x \, e^{-jk_z z}$$

$$H_y(x,y,z) = \left[V_0(y) \sqrt{\frac{1}{a}} + V_1(y) \sqrt{\frac{2}{a}} \sin \frac{\pi}{a} x \right] \frac{k_z}{k} \sqrt{\frac{\varepsilon}{\mu}} \, e^{-jk_z z}$$

$$H_z(x,y,z) = -\left[I_0(y) \sqrt{\frac{1}{a}} + I_1(y) \sqrt{\frac{2}{a}} \sin \frac{\pi}{a} x \right] e^{-jk_z z}$$

We should note that the field ratios

$$\frac{E_x}{H_y} = -\frac{E_y}{H_x} = \frac{k}{k_z} \sqrt{\frac{\mu}{\varepsilon}} = \frac{\omega\mu}{k_z} = Z_z$$

are equal to the characteristic impedance of the longitudinal TE mode (in the z direction), as expected. The specific values of the V and I terms depend on the location in the cross section, and are determined by the dispersion relation.

2. The Step Junctions

Two identical step junctions appear in the cross section of the antenna shown in Fig. 3, but the effect of a step junction on the i=1 and the i=0 transverse modes is different. We should also recognize that these step junctions do not couple the i=1 and i=0 modes. We thus require separate expressions for each of the two modes, corresponding respectively to boxes S_1 and S_0 in Fig. 4.

The step junction is a lossless asymmetric discontinuity, and it therefore requires three real quantities for its characterization. A useful equivalent circuit representation for that type of structure is the one shown in Fig. 5. It has been found by experience with careful measurements on a variety of step junction discontinuities in rectangular waveguide [14] that the series reactance X_s is always very small, and that for most situations it may be safely neglected. The representation in Fig. 5(b) thus conveniently reduces to a shunt network comprised of a shunt susceptance B and a transformer with turns ratio n.

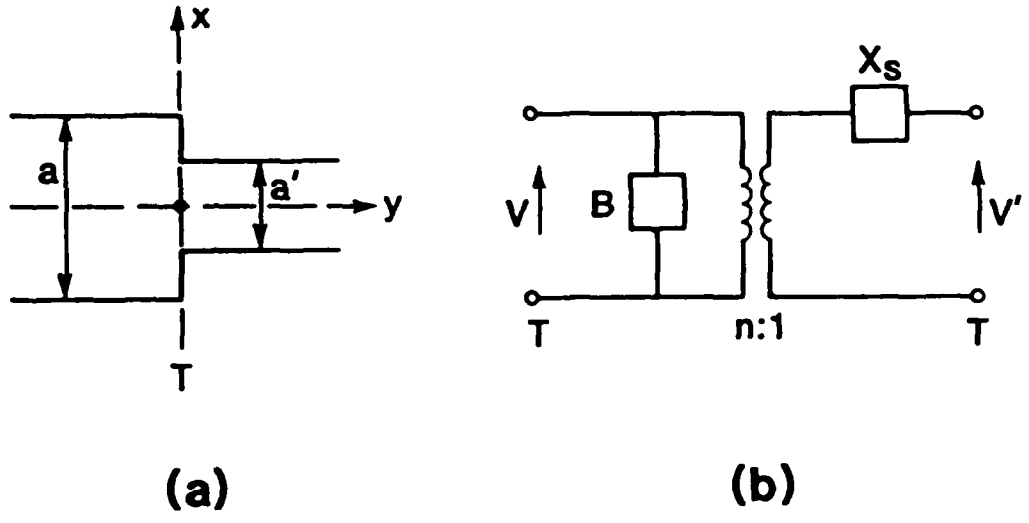

Fig. 5 The step junction and a rigorous equivalent circuit representation for it. For most steps, X_s is very small and can be neglected.

(a) The Transformer Turns Ratio

From the equivalent circuit in Fig. 5(b), after setting $X_s = 0$, we see that the transformer turns ratio is given simply by

$$n = \frac{V}{V'} \tag{12}$$

where the voltages V and V' are given by

$$V(0) = \int_{-a'/2}^{a'/2} \underline{E}_t(x,0,z) \cdot \underline{e}^*(x,z)dxdz \tag{13}$$

$$V'(0) = \int_{-a'/2}^{a'/2} \underline{E}_t(x,0,z) \cdot \underline{e}'^*(x,z)dxdz$$

if we choose y=0 to define the plane of the step junction shown in Fig. 5(a), and if the step is uniform along z. For simplicity, we choose the

aperture transverse electric field $\underline{E}_t$ to be the same as the mode field in the guide of narrower width, a'.

For the mode i=1, we would then write

$$\underline{E}_t(x,0,z) = E_a(x)e^{-jk_z z}\underline{x}_o = A \sin\frac{\pi x}{a'} e^{-jk_z z}\underline{x}_o \qquad (14)$$

On use of (7) for the mode function and relations (13) and (14), expression (12) for n simplifies to

$$n_1 = \frac{\int_{-a'/2}^{a'/2} \sqrt{\frac{2}{a}} \sin\frac{\pi x}{a} \sin\frac{\pi x}{a'}\, dx}{\int_{-a'/2}^{a'/2} \sqrt{\frac{2}{a'}} \sin^2\frac{\pi x}{a'} dx}$$

so that

$$n_1^S = \left[\frac{a'}{a}\right]^{3/2} \frac{4}{\pi} \frac{\cos\frac{\pi a'}{2a}}{1-(\frac{a'}{a})^2} \qquad (15)$$

where the superscript S, which we have just added, signifies "step".

Proceeding similarly for the i=0 mode, one finds, using (9) for the mode function,

$$n_0^S = \sqrt{\frac{a'}{a}} \qquad (16)$$

(b) The Shunt Susceptances

Since the fields for the i=1 and i=0 transverse modes are different, the step junction shunt susceptances will also be different. The normalized susceptance B_1/Y_1 for the i=1 mode has been derived previously in reference 15 in connection with the transverse equivalent network for the dominant mode alone. The expression is

$$\frac{B_1}{Y_1} = 0.55\, k_{y1} \frac{2a}{\pi} \cot\frac{2\pi a'}{2a} \qquad (17)$$

The factor 0.55 arises because (17) is obtained from an expression for the normalized susceptance of a zero-thickness transverse symmetrical window of relative aperture a'/a subjected to i=1 mode incidence. From stored power considerations, presented in reference 15, and from prior experience with careful measurements on step junctions of various types in rectangular waveguide [14], it was found that the factor 0.55 represents a good rule of thumb when extrapolating from a zero-thickness structure to a step junction of similar dimensions. The factor k_{y1} enters because it is the wavenumber of the transmission line in the y direction for the i=1 mode.

For the i=0 mode in the y direction, we can make use of expressions for the normalized susceptance available in the Waveguide Handbook [16]. One may use either an expression in Sec. 5.26 on pages 307 and 308, which applies directly to a step junction, or expression 2(a) of Sec. 5.1 on page 218, after multiplication by 0.55 for the reasons stated above. For convenience, we employ a simplified version of the latter expression. Our result for the normalized susceptance of the step junction when the i=0 mode is incident is

$$\frac{B_0}{Y_0} = 0.55\, k_{y0}\, \frac{2a}{\pi}\, \ell n\, \csc\, \frac{\pi a'}{2a} \tag{18}$$

Expressions (17) and (18) are seen to resemble each other somewhat, but they have different functional dependences with respect to a'/a. In the range of <u>small steps,</u> however, they are really more similar than they appear. They may be rewritten in the forms

$$\frac{B_1}{Y_1} = 0.55\, k_{y1}\, \frac{2a}{\pi}\, \tan^2\left[\frac{\pi}{2}\left(1 - \frac{a'}{a}\right)\right] \tag{19}$$

$$\frac{B_0}{Y_0} = 0.55\, k_{y0}\, \frac{2a}{\pi}\, \ell n\, \sec\left[\frac{\pi}{2}\left(1 - \frac{a'}{a}\right)\right] \tag{20}$$

which become, in the limit of a'/a→1 (small steps),

$$\frac{B_1}{Y_1} = 0.55\, k_{y1}\, \frac{\pi a}{2}\left(1 - \frac{a'}{a}\right)^2 \tag{21}$$

$$\frac{B_0}{Y_0} = 0.55\, k_{y0}\, \frac{\pi a}{4}\left(1 - \frac{a'}{a}\right)^2 \tag{22}$$

Both susceptances are seen to approach zero as the square of (a-a'), in agreement with what one obtains from small obstacle considerations.

3. The Asymmetrical Coupling Strip

We next derive the equivalent network for the asymmetrical strip of width δ (see Fig. 3) which couples the exciting i=1 transverse mode to the radiating i=0 transverse mode. We should also recall that the strip is located in the narrow parallel plate region of width a', where the i=1 transverse mode is below cutoff, so that the strip is excited by an evanescent field. Thus, the strip couples a propagating mode (i=0) and an evanescent mode (i=1).

A network which accurately describes such coupling for arbitrary values of δ/a might be rather involved, but we seek in our leaky wave antenna to produce small leakage per unit length, so that the radiated beams can be narrow. As a result, we are concerned primarily with small values of δ/a. It is appropriate therefore to employ a small obstacle approach, which results in a simple network representation for the coupling effects. The small obstacle formulation must be valid, however, in a multimode context, where one of the modes is below cutoff.

Fortunately, a formulation which supplies most of the requirements is available in the literature [17]. In addition, a very simple and convenient network form is presented that is valid for transverse obstacles, which is precisely our case. The requirement that is lacking is the condition that one of the modes is below cutoff, but the formulation can be modified easily to account for that added step.

The small obstacle approach considers that the fields incident on the small obstacle redistribute the surface charges such that equivalent electric and magnetic dipoles are created whose strengths are proportional to the electric and magnetic polarizabilities of the obstacles. This approach assumes that these polarizabilities can be computed under "static" conditions with the obstacle in "free space," meaning not near to any walls. The expressions for the polarizabilities are, as a result, very simple in form. One then computes the fields excited within the waveguide by the equivalent dipoles mentioned above, so that the waveguide mode functions enter into the calculations. The field components that are taken into account in determining the influence of the obstacle are the tangential component(s) of the electric field and the normal component of the magnetic field. For the asymmetrical strip

of width δ, the field components are E_x and H_y.

Small obstacle theory, as indicated above, assumes that the obstacle is far from the walls, but in our problem the coupling strip is located <u>at</u> a wall. It is necessary to employ symmetry to modify the cross section so as to satisfy this consideration. As seen in Fig. 6, the asymmetrical strip of width δ in a waveguide of width a' with the $i=1$ mode incident is equivalent to a centered symmetrical strip of width 2δ in a waveguide of width $2a'$ with the $i=2$ mode incident. The calculation is therefore made first for the latter set of specifications, and then the equivalence is used to adapt the result to the guide of width a'.

Reference 17 shows that the coupling network can take on the simple form appearing in Fig. 7 since the small obstacle is transverse. That reference also presents, in its Eq. (37), a simple approximate expression for the admittance element y_{ij} that couples two propagating modes in a multimode waveguide, namely,

$$y_{ij} = j\omega(\mu Y_i Y_j m\, h^*_{yio}\, h_{yjo} + \varepsilon\, \underline{e}^*_{io} \cdot P_t \cdot \underline{e}_{jo}) \tag{23}$$

In this expression, we have changed z to y, in conformity with our coordinate system in Fig. 3, and we have added the factor ω which reference 17 inadvertently omitted. The Y_i and Y_j represent the characteristic admittances for the two modes, m and P_t are the magnetic scalar and electric tensor polarizabilities, and h and e represent the magnetic and electric mode functions. The subscript o means that the value of the mode function is taken at the center of the obstacle, and the asterisk signifies complex conjugate. The particularly simple form in Fig. 7 means that y_{ij} can be written as

$$y_{ij} = y_{00}\, n_i^0\, n_j^0 \tag{24}$$

where the superscript 0 designates a turns ratio representative of the "obstacle," as distinguished from those for the step junctions. (It should be mentioned that in Fig. 5 of reference 17 the turns ratios should be specified as 1:n rather than n:1.)

When one of the modes that are coupled together is below cutoff, expression (23) must be modified by writing Y_i^* rather than Y_i, if the ith mode is the one below cutoff.

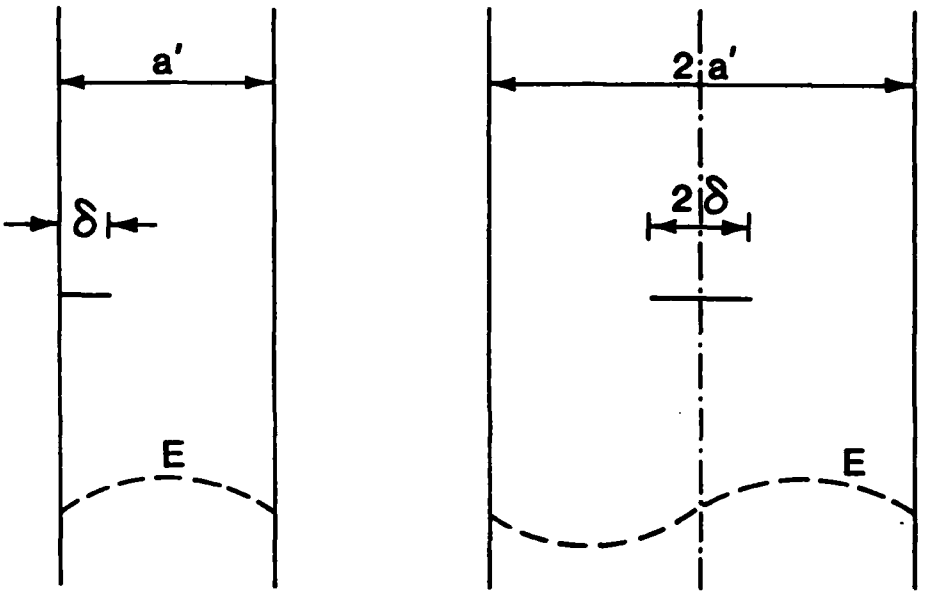

Fig. 6 Left: Actual guide with asymmetrical strip of width δ. Right: Equivalent double width guide with centered symmetrical strip of width 2δ.

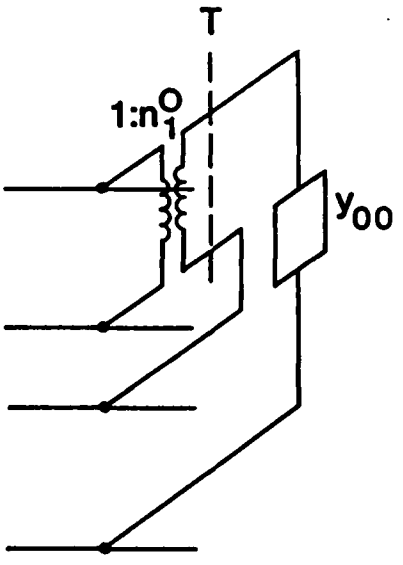

Fig. 7. Simple equivalent network, based on a small obstacle approach, for the asymmetrical strip that couples the bound i = 1 and the radiating i = 0 transverse modes.

For the asymmetrical strip, the field components required are E_x and H_y, so that expression (23) reduces to

$$y_{ij} = j\omega\mu m\, Y_i^* Y_j h_{yio}^* h_{yjo} + j\omega\epsilon p\, e_{xio}^* e_{xjo} \tag{25}$$

where $P_t = p\, \underline{x}_o\, \underline{x}_o$, and we have added the complex conjugate designation on Y_i. The polarizabilities for a long strip of width d are

$$p = -m = \pi(d/2)^2 \tag{26}$$

per unit length of strip, in the notation of reference 17, and used above. From Fig. 6(b) we see that $d/2 = \delta$, so that

$$p = -m = \pi\delta^2 \tag{27}$$

The mode functions for the i=2 mode in the waveguide of width 2a', as in Fig. 6, are obtained in a manner identical to those given above for i=1, in Eqs. (7) and (8), subject to normalization (5). They are

$$e_{x2}(x,z) = \sqrt{\frac{1}{a'}} \cos\frac{\pi x}{a'}\, e^{-jk_z z} \tag{28}$$

$$h_{y2}(x,z) = \sqrt{\frac{1}{a'}} \frac{k_{y2}k_z}{k^2-k_z^2} \cos\frac{\pi x}{a'}\, e^{-jk_z z} \tag{29}$$

which are then taken at x=0 when used in (25). Similarly, the mode functions for the i=0 mode in the waveguide of width 2a become

$$e_{x0}(x,z) = \sqrt{\frac{1}{2a'}}\, e^{-jk_z z} \tag{30}$$

$$h_{y0}(x,z) = \sqrt{\frac{1}{2a'}} \frac{k_z}{k_{y0}}\, e^{-jk_z z} \tag{31}$$

The values of k_z and k_{y0} above are the same as those for the waveguide of width a', while k_{y2} for the guide of width 2a' is the same as k_{y1} for the guide of width a'. In this problem, k_z and k_{y0} are real and k_{y2} is imaginary.

Since k_{y2} and Y_2 in the guide of width 2a' are equal to k_{y1} and Y_1 in the original guide of width a', and since k_{y0} and Y_0 are the same in both guides, we may insert the coupling network in Fig. 7 directly into

the transverse equivalent network in Fig. 4 after identifying the appropriate equivalences in the results obtained from Eq. (25). In using (25), however, we shall assume that the two modes involved are the i=0 and i=2 modes in the guide of width 2a'; subsequently, the equivalences will be made to adapt the results to the original i=0 and i=1 modes.

Although either y_{00} or y_{22} can be used in the coupling network, we have chosen y_{00}. When the mode functions in (30) and (31), and relations (11) and (27), are inserted into (25), one obtains

$$y_{00} = j \frac{\pi\delta^2}{2a'} \frac{k_{y0}^2}{\omega\mu} \tag{32}$$

since $k^2-k_z^2 = k_{y0}^2$. The turns ratio n_2^0 is obtainable from (24) as

$$y_{22} = y_{00}(n_2^0)^2 \tag{33}$$

so that y_{22} must also be derived. Using (28), (29), (2) and (27) in (25), we find

$$y_{22} = j \frac{\pi\delta^2}{a'} \frac{k^2 - k_z^2}{\omega\mu} \tag{34}$$

which differs from y_{00} in (32) by only a factor of 2. From (33), (32) and (34), we thus deduce that

$$n_2^0 = \sqrt{2} \tag{35}$$

In view of the equivalences mentioned earlier, and the forms of y_{00} and n_2^0, we can now identify y_{00} and n_2^0 as computed above with the y_{00} and n_1^{02} required in Fig. 7, and directly employ relations (32) and (35).

The simple form of Fig. 7 is a familiar one in equivalent network formulations, and it requires that the condition $y_{00}\, y_{22} - y_{02}^2 = 0$ be satisfied. On use of (25), one finds readily that the condition indeed applies here. That formulation also indicates that the turns ratio n_2^0 is given by

$$n_2^0 = \frac{y_{02}}{y_{00}} \tag{36}$$

Again, from (25) and (36) one readily verifies that (35) is correct. The coupling network in Fig. 7 is therefore self-consistent and valid in the small-obstacle limit.

4. The Radiating Open End

In the narrower regions of the groove guide, of width a', the i=1 transverse mode is evanescent and the i=0 transverse mode is propagating. The length c", shown in Fig. 3, is assumed to be sufficiently long that the fields in the evanescent i=1 mode have decayed to negligible values as they reach the open end. In the transverse equivalent network, whose form is presented in Fig. 4, the i=1 transmission line is therefore taken to be infinite, and a box labeled Y_R is placed at the end of the i=0 transmission line to represent the admittance effect of the open end on that propagating mode.

For box Y_R in Fig. 4, we require the equivalent circuit for a TE mode (which is what the $H^{(z)}$-type i=0 mode reduces to) incident in the y direction on an open-ended parallel plate guide of width a', with the electric field perpendicular to the plates. Such an equivalent circuit is already available in the Waveguide Handbook [16], on page 179, in the form of a susceptance and a conductance in parallel across the end of the transmission line. Our notation differs in minor ways from that in the Waveguide Handbook, but we employ Eqs. (3) and (4), together with (1) and part of (2), on page 179. The biggest difference is that their λ' becomes our $2\pi/k'_{y0}$. Our admittance, comprised of $G_R + jB_R$, where the subscript R signifies "radiating," is taken directly at the open end, corresponding to their reference plane T'.

In our notation, the relevant relations become

$$\frac{G_R}{Y'_0} = \frac{\sinh (k'_{y0}a'/2}{\cosh (k'_{y0}a'/2) + \cos 2k'_{y0}d} \tag{37}$$

$$\frac{B_R}{Y'_0} = \frac{\sin 2k'_{y0}d}{\cosh (k'_{y0}a'/2) + \cos 2k'_{y0}d} \tag{38}$$

where

$$2k'_{y0}d = k'_{y0}\frac{a'}{\pi} \ell n \frac{4\pi e}{\gamma k'_{y0}a'} - 2S_1(k'_{y0}\frac{a'}{2\pi};0,0) \tag{39}$$

with e = 2.718, γ=1.781, and

$$S_1(t;0,0) = \sum_{n=1}^{\infty} \left(\sin^{-1}\frac{t}{n} - \frac{t}{n}\right) \tag{40}$$

The above relations have been obtained by the transform method, and are rigorous in the range $k'_{y0}a'/2\pi < 1$. We have found, however, that the values of $k_z = \beta - j\alpha$ computed via the transverse equivalent network are affected negligibly when the infinite sum S_1 in (40) is replaced by its first term only. We have therefore replaced (40) by

$$S_1(t;0,0) \cong \sin^{-1}t - t \tag{41}$$

in our dispersion relation.

5. The Complete Transverse Equivalent Network

In subsections 1 through 4 above, we have presented expressions for all the constituents of the transverse equivalent network whose basic form appeared in Fig. 4. The final form of that network is now presented in Fig. 8.

The two transmission lines comprising the network in Fig. 8 represent the transverse i=1 mode, which is the exciting mode, and the transverse i=0 mode, which is the mode created by the added coupling strip and which produces the radiation. Both transverse modes propagate in the y direction, and they combine to produce the net longitudinal TE mode in the z direction, with propagation constant $k_z = \beta - j\alpha$, the value of α representing the leakage per unit length from the radiating open end. As mentioned earlier, the transverse equivalent network in Fig. 8 is descriptive of the cross section of the antenna structure in Fig. 3, but it is placed on its side for clarity.

The propagation wavenumbers in the two transverse transmission lines are related to k_z by

$$k_{y1}^2 = k^2 - k_z^2 - (\pi/a)^2 \tag{42}$$

$$(k'_{y1})^2 = k^2 - k_z^2 - (\pi/a')^2 \tag{43}$$

$$k_{y0}^2 = k^2 - k_z^2 = (k'_{y0})^2 \tag{44}$$

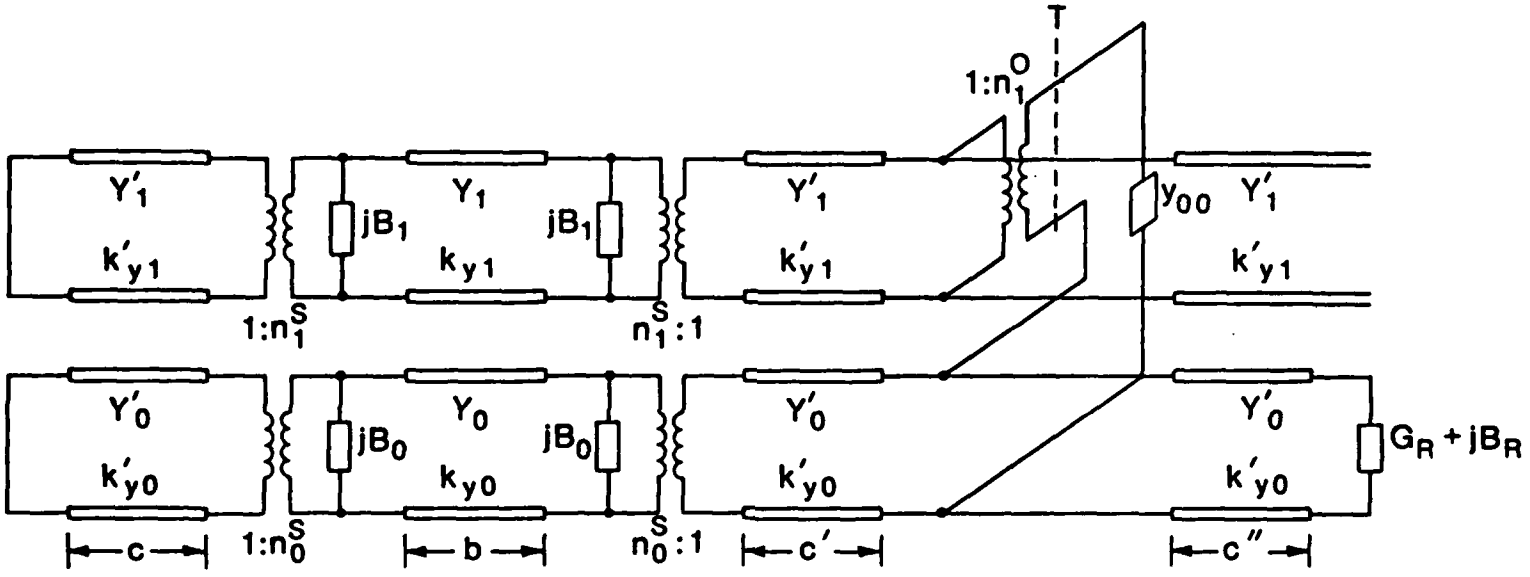

Fig. 8 Complete transverse equivalent network for the structure whose cross section is shown in Fig. 3.

Wavenumbers k_{y1}, k_{y0} and k'_{y0} are basically real, and k'_{y1} is basically imaginary. The characteristic admittances are related to the respective wavenumbers by (2), although those for the i=0 line can employ the simpler form (11) in view of (44).

Boxes S_1 and S_0 in Fig. 4, representing the effect of the step junctions on the i=1 and i=0 modes, respectively, take the form in Fig. 8 of shunt susceptances B_1 and B_0 together with ideal transformers of turns ratios n_1^S and n_0^S. Expressions for the shunt susceptances B_1/Y_1 and B_0/Y_0, normalized to their respective characteristic admittances, are given by (17) and (18), or in alternative forms (19) and (20). The turns ratios appear in (15) and (16).

The terminal admittance $G_R + jB_R$, representing the effect of the open end on the radiating i=0 transmission line, is described by relations (37) and (38), together with (39) and (41).

The influence of the added coupling strip in Fig. 3 is expressed in basic form by the box labeled Ob, representing "obstacle," in Fig. 4, and more explicitly by the simple network in Fig. 7. The network in Fig. 7 is then employed as part of the overall network in Fig. 8. Expressions for the parameters y_{00} and n_1^0 of this coupling network are presented in (32) and (35); the discussion there explains why n_1^0 and n_2^0 are the same in the context of (35).

We are pleased that we were able to obtain all of the constituents of the transverse equivalent network in Fig. 8 in closed form. Despite the simple closed-form nature of the expressions for the step junction and the radiating open end, those expressions are believed to be sufficiently accurate to yield reliable numerical results for the propagation behavior of the leaky groove guide antenna. The coupling network representing the added asymmetrical strip was derived using small obstacle theory, and was found to be self-consistent and valid for small values of strip width δ. The results for $\beta - j\alpha$ for small strip widths should therefore be quite accurate, but the leakage rate α would be small for narrow strips, resulting in a long antenna and therefore a rather narrow radiated beam. From other considerations, which are touched upon in Section E, we believe that for wider strips the leakage rate is actually greater than that computed using the small obstacle approach. In other words, the actual strip width required for a wider beam is somewhat smaller than that indicated by the theory, meaning that the range of practical beam widths is greater than that predicted by the

theory under the small obstacle assumption.

The last feature to note in connection with Fig. 8 is the location of reference plane T. The dispersion relation presented in Section D was obtained by applying the transverse resonance condition to this network at reference plane T.

D. THE DISPERSION RELATION

1. The Dispersion Equation

The dispersion relation yields, as a function of frequency and the dimensional parameters, the behavior of the phase constant β and the attenuation constant α of the longitudinal TE mode that propagates along the z direction in Fig. 3. From this information the leaky wave antenna can be designed according to prescribed specifications. The relations among the frequency (or free space wavenumber k, since $k = 2\pi f/c$), the longitudinal wavenumber $k_z = \beta - j\alpha$, and the transverse wavenumbers are given in (42) to (44). The transverse wavenumbers k_{y1}, k'_{y1} and k_{y0} $(=k'_{y0})$ are related by a dispersion equation that is readily derivable from the transverse equivalent network in Fig. 8 upon application of the transverse resonance condition

$$\overrightarrow{Y}(T) + \overleftarrow{Y}(T) = 0 \tag{45}$$

Since relation (45) represents a free resonance, reference T may be chosen anywhere in the network; our choice is indicated in Fig. 8.

The application of (45) to the transverse equivalent network in Fig. 8 yields the dispersion equation (46) shown on the next page.

The dispersion behavior is then obtained from this equation and those in (42) to (44), also recognizing that $Y'_0 = Y_0$.

2. Numerical Procedure

By following the numerical procedure given by Bardati and Lampariello [18], the roots of the complete transcendental dispersion equation (46) on the complex plane have been found when parameters such as the frequency f, the width b of the groove, the length c" of the upper part of the waveguide, and others, are varied.

The whole equation (46) can be regarded as an implicit function of two variables set equal to zero:

$$W(z,p) = 0$$

where z is the actual unknown $k_{y1}b$, and p stands for the parameter which is to be varied. The problem of finding the roots of this equation is

$$\frac{k_{y0}^2}{(n_1^{O})^2 k'_{y1}} \frac{\left\{(n_1^{S})^2\left[k_{y1}\,0.55\frac{2a}{\pi}\cot^2\left(\frac{\pi a'}{2a}\right)+\frac{\left(k_{y1}\,0.55\frac{2a}{\pi}\cot^2\left(\frac{\pi}{2}\frac{a'}{a}\right)-\frac{1}{(n_1^{S})^2}\frac{k_{y1}}{k'_{y1}}\cot k'_{y1}c\right)\cot k_{y1}b+1}{\cot k_{y1}b-\left(k_{y1}\,0.55\frac{2a}{\pi}\cot^2\left(\frac{\pi}{2}\frac{a'}{a}\right)-\frac{1}{(n_1^{S})^2}\frac{k_{y1}}{k'_{y1}}\cot k'_{y1}c\right)}\right]-j\frac{k_{y1}}{k'_{y1}}\right\}(j\cot k'_{y1}c'-1)}{\frac{k_{y1}}{k'_{y1}}\cot k'_{y1}c'-(n_1^{S})^2\left[k_{y1}\,0.55\frac{2a}{\pi}\cot^2\left(\frac{\pi}{2}\frac{a'}{a}\right)+\frac{\left(k_{y1}\,0.55\frac{2a}{\pi}\cot^2\left(\frac{\pi}{2}\frac{a'}{a}\right)-\frac{1}{(n_1^{S})^2}\frac{k_{y1}}{k'_{y1}}\cot k'_{y1}c\right)\cot k_{y1}b+1}{\cot k_{y1}b-\left(k_{y1}\,0.55\frac{2a}{\pi}\cot^2\left(\frac{\pi}{2}\frac{a'}{a}\right)-\frac{1}{(n_1^{S})^2}\frac{k_{y1}}{k'_{y1}}\cot k'_{y1}c\right)}\right]}+$$

$$+\frac{1}{\frac{1}{j\frac{\pi\delta^2}{2a'}k_{y0}^2}+\frac{1}{\frac{1}{(n_0^{O})^2}k_{y0}\left\{j\frac{(n_0^{S})^2\left[k_{y0}\,0.55\frac{2a}{\pi}\ln\left(\csc\frac{\pi}{2}\frac{a'}{a}\right)+\frac{\left(k_{y0}\,0.55\frac{2a}{\pi}\ln\left(\csc\frac{\pi}{2}\frac{a'}{a}\right)-\frac{1}{(n_0^{S})^2}\cot k_{y0}c\right)\cot k_{y0}b+1}{\cot k_{y0}b-\left(k_{y0}\,0.55\frac{2a}{\pi}\ln(\csc\frac{\pi}{2}\frac{a'}{a})-\frac{1}{(n_0^{S})^2}\cot k_{y0}c\right)}\right]\cot k_{y0}c'+1}{\cot k_{y0}c'-(n_0^{S})^2\left[k_{y0}\,0.55\frac{2a}{\pi}\ln(\csc\frac{\pi a'}{2a})+\frac{\left(k_{y0}\,0.55\frac{2a}{\pi}\ln(\csc\frac{\pi}{2}\frac{a'}{a})-\frac{1}{(n_0^{S})^2}\cot k_{y0}c\right)\cot k_{y0}b+1}{\cot k_{y0}b-\left(k_{y0}\,0.55\frac{2a}{\pi}\ln(\csc\frac{\pi}{2}\frac{a'}{a})-\frac{1}{(n_0^{S})^2}\cot k_{y0}c\right)}\right]}+R\right\}}}=0$$

$$\text{where } R=\frac{k_{y0}\frac{a'}{4}\left[1+j\frac{2}{\pi}\ln\left(\frac{e}{\gamma}\frac{4\pi}{a'}\frac{1}{k_{y0}}\right)\right]\cot k_{y0}c'+j}{\cot k_{y0}c'+jk_{y0}\frac{a'}{4}\left[1+j\frac{2}{\pi}\ln\left(\frac{e}{\gamma}\frac{4\pi}{a'}\frac{1}{k_{y0}}\right)\right]}$$

Equation (46)

that of making explicit the implicit function as a function z of the parameter p:

$$z = z(p)$$

If one root of the equation, say z_o for a given value of the parameter p_o, is known on the basis of the implicit function theorem [19], another root z exists inside a circle with center at z_o for a different value of the parameter $p = p_o + \Delta p$. The circle should be sufficiently small so as to contain only one root for each of the values p_o and $p_o + \Delta p$ of the parameter.

Using this procedure, let us assume that we know the zeros of the transverse resonance equation for the i=1 mode when the coupling strip is absent and the length c" of the upper part of the waveguide is infinite. Now, let us write

$$W(z,h) = A(z) + \frac{h}{B(z)} = 0 \qquad (47)$$

where A(z) is the function that refers to the above-mentioned i=1 mode. The zeros of this equation are identical to those of the complete transverse resonance equation when the parameter h is set equal to unity. Starting from the known root of the equation for h=0, it is possible to calculate the final solution by varying the parameter h from 0 to 1. If we consider the function $[W(z,h)]_{h=1}$ as a function of any other parameter which is of interest to be varied, the frequency for example, the equation

$$W(z,f) = 0$$

can be solved starting from the now known root for a given frequency; that is, the explicit function.

$$z = z(f)$$

can be numerically constructed.

It is worthwhile to note that the numerical method employed for solving transcendental equations [20] provides roots with very high precision. For the function arising here, the real and the imaginary parts of the function calculated at the zero are at least 12 orders of magnitude lower than the minimum value of the modulus of the function along a

circumference with center at the zero and with a very small radius.

E. NUMERICAL VALUES AND DESIGN CONSIDERATIONS

1. Some General Properties of Leaky Wave Antennas

In order to place the numerical values to be presented below in proper context, it is important to recall a few general properties of leaky wave antennas.

A leaky wave antenna is basically an open waveguide possessing a mechanism which permits a slow leakage of power along the length of the waveguide. The leaky wave that exists at the opening along the length of the waveguide provides the aperture field distribution of the antenna, and the length of the waveguide over which the leaky wave contains significant power defines the antenna aperture length. It is customary to retain a length for which 90% or 95% of the power can leak away; the remaining 10% or 5% is absorbed in a load placed at the end of the waveguide.

The rate of leakage per unit length along the waveguide is given by the attenuation constant α of the complex propagation constant $k_z(=\beta-j\alpha)$ of the leaking waveguide mode. If the value of α is small, the antenna aperture will be long, and the far field radiation pattern will possess a narrow beam. If α is large, the power is radiated more rapidly along the antenna length and a wider radiated beam will be obtained.

The design of a leaky wave antenna proceeds by first specifying the desired performance characteristics of the antenna: the angle of maximum radiation, the beam width, and the side lobe properties. The angle θ_m that the maximum of the main beam makes with the normal to the antenna aperture (broadside direction) is given approximately by

$$\sin \theta_m \cong \beta/k = \lambda/\lambda_g \tag{48}$$

where β is the phase constant of the complex propagation constant k_z. The beam width $\Delta\theta$ is related linearly to the reciprocal of the aperture length L, and a rule of thumb for $\Delta\theta$ is

$$\Delta\theta \cong \frac{\lambda}{L \cos \theta_m} \tag{49}$$

Relation (48) above is summarized pictorially in Fig. 9.

For the side lobe properties, it is well known that the antenna

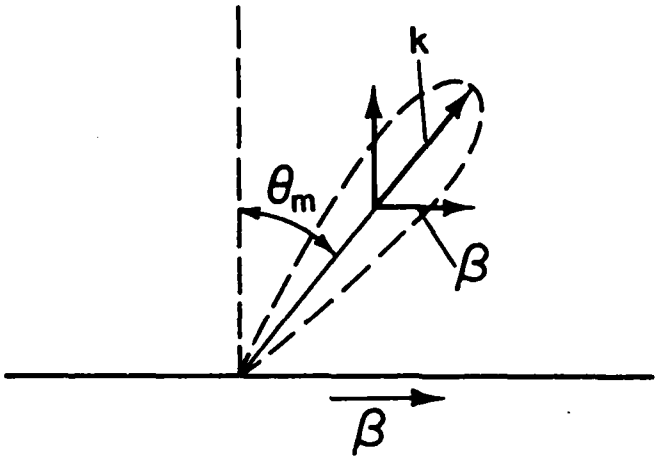

Fig. 9 Pictorial representation for $\sin \theta_m \cong \beta/k$, where θ_m is the angle that the maximum of the radiated beam makes with the normal to the antenna aperture surface, and β is the phase constant of the leaky wave that travels along the aperture surface.

aperture distribution must be tapered in a specified fashion in order to achieve the desired side lobe requirements. The necessary tapers corresponding to various side lobe specifications appear in standard antenna texts. When the aperture distribution is tapered, relation (49) for the beam width is affected somewhat numerically, but not more than ±25% depending on the taper, so that (49) remains a useful and reasonably accurate indication of the beam width.

When the geometry of the waveguide is uniform along its length, the aperture distribution consists of a slow exponential decay. To produce the taper needed for the side lobe requirements, it is necessary to vary the α of the waveguide along the length L, and therefore to vary the transverse dimensions in some fashion along the waveguide length. The phase constant β is maintained constant along the length so that all parts of the antenna aperture radiate at the same angle θ_m. The relation between $\alpha(z)$, where z is the longitudinal coordinate, and the desired taper along z of the antenna aperture distribution is also

available in the literature.

The dispersion relation (46) for the leaky groove guide yields the values of α and β corresponding to specific geometrical parameters in the cross section. That relation must be used in a specific design to produce the $\alpha(z)$ needed while maintaining $\beta(z)$ constant. Part of the design considerations to be presented below are aimed at recommending which geometrical parameter or parameters should be varied to change α but not β.

The remainder of the report discusses the behavior of the leaky groove guide when the cross section is maintained constant, and it stresses the variation of β and α with frequency and with various dimensional parameters. If we assume, as is common, that the antenna aperture of length L radiates 90% of the power (with the remaining 10% absorbed by a load), then the power level at the end of the antenna aperture is 10 dB down from its value at the beginning. In the numerical values that follow, we shall present the α value in the form α/k in nepers, so that the value of α in dB per wavelength is $2\pi(8.686)(\alpha/k) = 54.6\ (\alpha/k)$. The antenna length L in free space wavelengths is then approximately

$$\frac{L}{\lambda} \simeq \frac{10}{54.6}\,\frac{1}{\alpha/k} \simeq \frac{0.18}{\alpha/k} \tag{50}$$

The precise value of L will depend on how the aperture distribution is tapered. If the percentage of power radiated is different from 90%, the length L in (50) will differ somewhat numerically, but may be readily computed.

In summary, the values of β/k and α/k that are presented below permit us to determine readily the values of θ_m from (48), the aperture length L from (50), and the beamwidth $\Delta\theta$ from (49).

2. Optimization and Other Design Considerations

In order to systematically design radiation patterns, one must be able, as explained in the section just above, to taper the antenna aperture amplitude distribution while maintaining the phase linear along the aperture length, i.e., one must be able to vary α while keeping β the same. Fortunately, several parameters can be varied that will change α while affecting β hardly at all; those parameters are δ, c, c' and c", as is evident from the numerical values given in the next section.

Practical considerations may rule out parameters δ and c'; lengths c and c" must be large enough that changing them does not affect the evanescent field distribution of the i=1 transverse mode.

In the design, one first chooses the width a and adjusts a' and b to achieve the desired value of β/k, which is determined essentially by the i=1 transverse mode. That value of β/k immediately specifies the angle of the radiated beam. It is then recognized that the value of α can be increased if the coupling strip width δ is increased, or if the distance c' between the step junction and the coupling strip is decreased, since the coupling strip is excited by the i=1 transverse mode, which is evanescent away from the step junction in the outer regions.

The selection of the values of the remaining dimensional parameters, c and c", requires special considerations. Since the i=0 transverse mode is <u>above</u> cutoff in both the central and outer regions of the guide cross-section, a <u>standing wave</u> effect is present in the i=0 transmission line. As a result, a short circuit can occur in that transmission line at the position of the coupling strip of width δ, and the value of α then becomes zero. Hence, we must choose the dimensions to avoid that condition, and in fact to optimize the value of α. Therefore, after c' is specified, the length c must be determined such that the standing-wave effect mentioned above optimizes the value of α. If c is sufficiently long, it will affect only the i=0 transmission line and influence β negligibly. The length c" also affects α strongly and β weakly, and it also must be optimized because another, although milder, standing wave exists between the coupling strip and the radiating open end.

It is important to realize that the dimensions for optimization are <u>independent of frequency,</u> since the transverse wavenumbers are all frequency independent. Of course, when the frequency is altered the values of β and α will change, but the dimensional optimization remains undisturbed.

The frequency-independent nature of the dimensional optimization can be put to practical advantage. Suppose that a curve of α/k vs. c' and the corresponding curve of α/k vs. c, where the values of c are optimized, have been obtained for a given frequency f_1. If now similar curves are desired for a second frequency f_2, it is not necessary to repeat the optimization calculations. One simply takes a curve of α/k

vs. frequency, and finds the ratio R of α/k at each of the two frequencies f_2 and f_1. The new values of α/k at frequency f_2, as a function of c' and c, are found simply by taking the values of α/k for f_1 at each of the c' and c values and multiplying each of them by the ratio R.

The frequency-independent property of the transverse wavenumbers leads to another simple relation which may sometimes be of value. By taking the imaginary parts of the wavenumber relation

$$\alpha\beta = \mathrm{Im}(k_{y1})\mathrm{Re}(k_{y1}) \tag{51}$$

where $k_z = \beta - j\alpha$ and $k_{y1} = \mathrm{Re}(k_{y1}) + j\ \mathrm{Im}(k_{y1})$, or

$$\frac{\alpha}{k} = \frac{C}{k^2}\frac{1}{\beta/k} \tag{52}$$

where C is a factor independent of frequency since k_{y1} is frequency independent. Relation (52) may be useful if the values of α/k and β/k are known at a given frequency, and the value of α/k is desired at another frequency. Accurate values of β/k are obtainable from the complete dispersion relation (46), but approximate values can be found from the much simpler expression

$$\cot k_{y1}\frac{b}{2} = \frac{1}{(n_1^S)^2}\frac{k_{y1}}{|k'_{y1}|} + \frac{B_1}{Y_1} \tag{53}$$

where n_1^S and B_1/Y_1 are given by (15) and (17); (53) is obtained by removing the coupling strip and making c and c' infinitely long, so that k_{y1} and $|k'_{y1}|$ become purely real here. An approximate value of α for a new frequency f_2 can then be determined using relation (52), where the value of C is obtained from the α/k and β/k values at the given frequency f_1. Alternatively, (52) may be rephrased as

$$(\alpha/k)_{f_2} = \frac{f_1^2}{f_2^2}\left[\frac{(\beta/k)_{f_1}}{(\beta/k)_{f_2}}\right](\alpha/k)_{f_1} \tag{54}$$

A third consequence of the frequency independence of the transverse wavenumbers is that the <u>beam width</u> of the radiation remains essentially <u>constant</u> as the beam is scanned by varying the frequency. Since

$$\cos^2\theta_m = 1-\sin^2\theta_m = 1-(\beta/k)^2$$

using (48), and

$$1-(\beta/k)^2 = (k_{y1}/k)^2 + (\pi/ka)^2 = (k_{t1}/k)^2$$

using (42), we may rewrite (49) as

$$\Delta\theta = \frac{\lambda}{L}\frac{k}{k_{t1}} \tag{55}$$

where k_{t1} is the transverse wavenumber corresponding to the i=1 transverse mode. In the rephrasing of (42) above, the value of α is set equal to zero, so that k_{y1}, and therefore k_{t1}, become purely real. Since k_{t1} is frequency independent, and $k = 2\pi/\lambda$, we see that the beam width becomes

$$\Delta\theta = \frac{2\pi}{Lk_{t1}} \tag{56}$$

which is independent of frequency.

3. Numerical Results

Using the numerical procedure described in Section D,2 to obtain numerical values from the dispersion relation (46), we have obtained numerical values in graphical form of the variation of α/k and β/k with each of the dimensional parameters. We report here a set of curves for a typical set of dimensions.

Consistent with the discussion in the preceding section on design considerations, we begin with the width ratio $a'/a = 0.68$ and a height $b/a = 0.40$ for the central region of the groove guide (see Fig. 3). These two dimensional parameters are the principal ones that determine the value of β/k. To obtain a reasonably large value of α/k, we choose a strip width $\delta/a = 0.25$ and its location $c'/a = 0.20$. Then, for a relative wavelength $\lambda/a = 1.20$, we found that the length c/a had to be 1.28 for optimization. The corresponding optimized value of c"/a turned out to be 1.50. These optimization considerations are discussed in subsection 2.

Curves of β/k and α/k as a function of fa (where f is the frequency in GHz and a is the width of the central region), corresponding to the

above set of normalized dimensions, are presented in Figs. 10(a) and (b). Figure 10(a) is replotted in Fig. 11 with β/k replaced by θ_m, the angle of the maximum of the radiated beam (see Fig. 9). The relative wavelength $\lambda/a = 1.20$, mentioned above, corresponds to $fa = 25$ in these figures. It is seen that the β and α values vary over a wide range, with particular sensitivity near cutoff. For these dimensions, the radiated beam can be scanned with frequency from about 15° to nearly 60° from the normal before the next mode begins to propagate.

In order to determine the variation of β/k and α/k with the dimensional parameters, we must select a specific value of fa, or λ/a. The value $\lambda/a = 1.20$ mentioned earlier (corresponding to $fa = 25$) is seen from Fig. 10(b) to yield a reasonably large value of α/k, and yet not be too close to cutoff. For guide width $a = 5.0$ mm, this relative wavelength corresponds to a frequency of 50 GHz.

In Fig. 12(a), we present a curve of α/k vs. c'/a, the normalized distance of the asymmetric strip from the step junction, corresponding to the relative wavelength $\lambda/a = 1.20$. As expected, small changes in c' produce large variations in α. It is next necessary to find the values of c/a, the normalized length of guide between the lower step junction and the short-circuited bottom of the groove guide, in accordance with the optimization discussed under 2. The optimization curve of α/k vs. c/a is shown in Fig. 12(b). In effect, this curve indicates the value of c/a required once α/k, via c'/a, is specified. It is interesting to note that the value of $c/a + c'/a$ required for optimization is nearly constant, so that a curve of α/k vs. $(c+c')/a$, as in Fig. 12(c), may be used as an alternative to that in Fig. 12(b).

In order to be sure that higher mode coupling between the discontinuities produced by the asymmetric coupling strip and the step junction is acceptably low, we determined the decay rate of the i=2 transverse mode. Under the conditions discussed here, it was found that $|k'_{y2}|/a = 0.82$, so that the field of that mode has decayed to less than 0.2 of its original value over the distance $c'/a = 0.20$. All the other higher modes decay much more rapidly. The i=2 mode contains only a small portion of the stored energy, however, so that the coupling strip discontinuity can safely be regarded as isolated with respect to the higher modes. The step discontinuity, moreover, does not even excite this transverse mode; the lowest higher mode permitted by its symmetry is the i=3 mode, which decays much more rapidly. We are thus safe in using the network in Fig. 8.

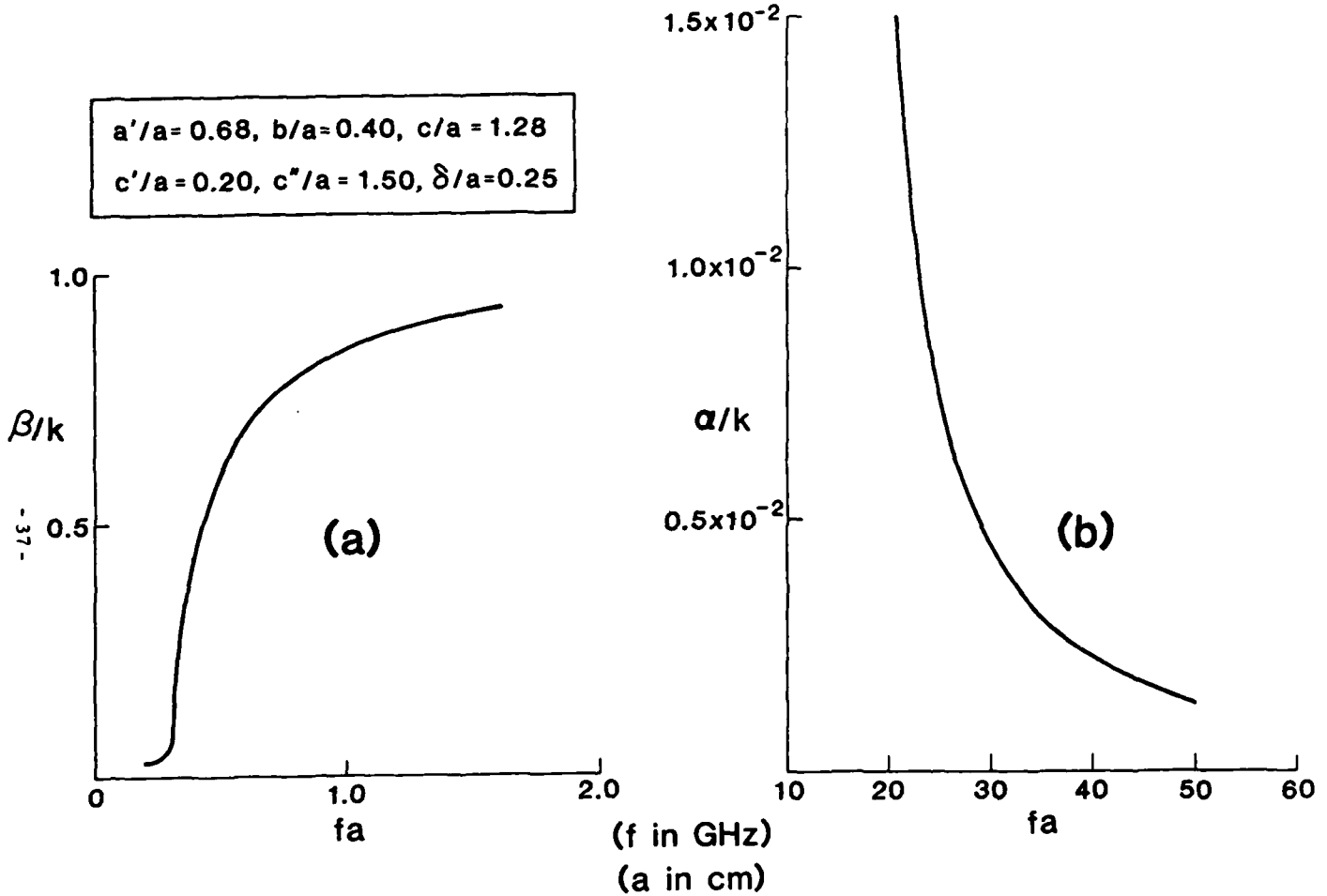

Fig. 10 Variation of normalized phase constant β/k and leakage constant α/k with normalized frequency in the form fa, where f is the frequency in GHz and a is the width of the guide's central region (see Fig. 3). The other geometrical parameter values are given in the box in the figure.

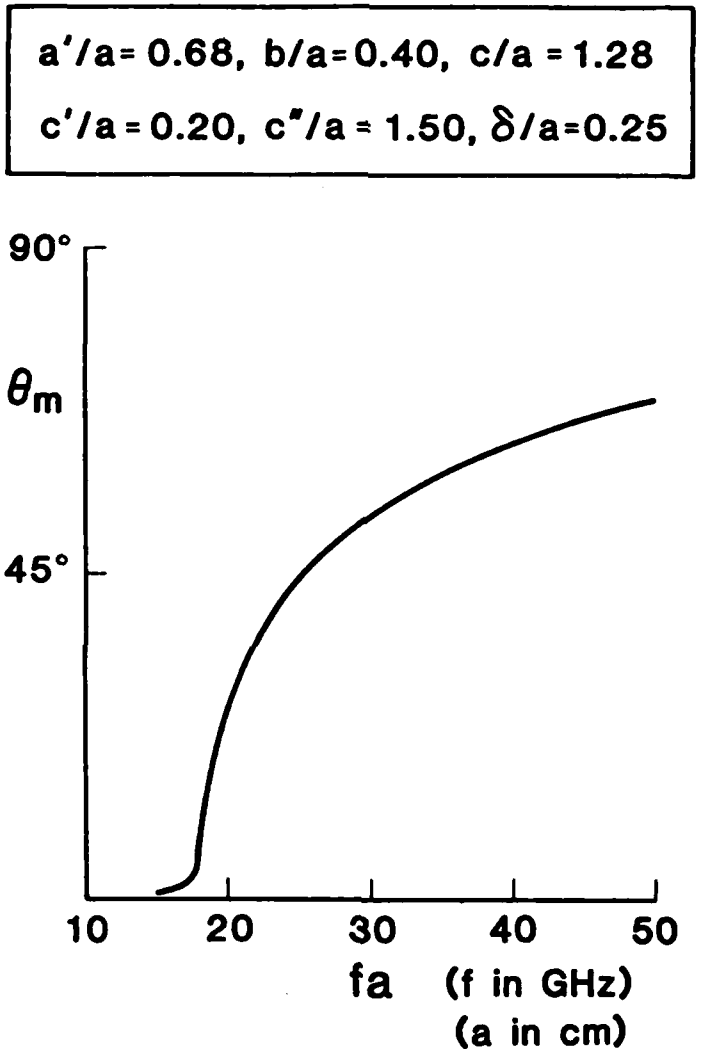

Fig. 11 Variation of the angle θ_m of the maximum of the radiated beam with the normalized frequency fa, defined as in Fig. 10.

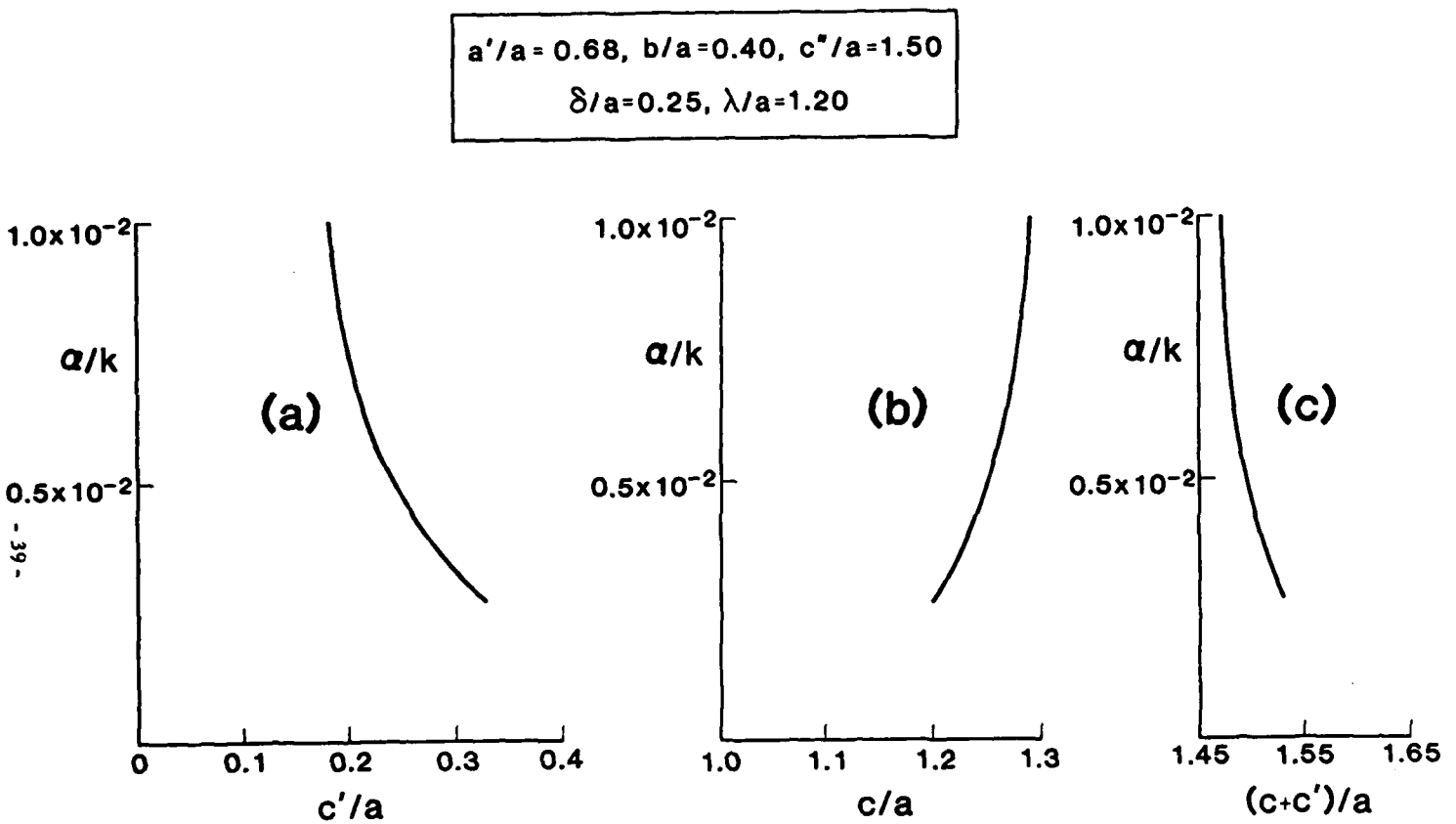

Fig. 12 (a) The variation of the normalized leakage constant α/k of the leaky wave antenna shown in Fig. 3 as a function of c'/a, the normalized distance of the perturbing asymmetric strip from the step junction. (b) The corresponding values of c/a required to optimize the values of α/k, where c is the length of guide between the lower step junction and the bottom of the groove guide. (c) An alternative phrasing for the dimensions for optimization, in terms of the sum $(c+c')/a$. The values of the normalized wavelength and the other dimensions are given in the box.

The variations of β/k and α/k with the normalized groove guide height b/a are shown in Fig. 13(a) and (b), where λ/a is taken as 1.20, and the other dimensions are the ones given earlier, including the optimization indicated in Figs. 12. It is seen that β/k varies considerably with b/a, particularly for smaller b/a values. The leakage constant α/k also varies strongly with b/a, showing a maximum value at about $b/a = 0.34$, rather that the 0.40 value taken above (and below) in connection with other figures. It is therefore possible to produce an additional optimization, by changing the value of b/a used in the determination of Figs. 12 from 0.40 to 0.34, but the increase in α/k will not be large. It is also seen that α/k becomes zero in the neighborhood of $b/a = 1.4$. The reason for this zero is that a null in the standing wave for the i=0 transverse mode, which is above cutoff in both the a and a' regions, then occurs exactly at the location of the asymmetric strip, thereby shorting out the coupling between the i=0 and the i=1 transverse modes.

The dependences of β/k and α/k on the normalized length δ/a of the asymmetric coupling strip are shown in Fig. 14(a) and (b). As expected, α/k depends very strongly on δ/a, whereas β/k changes hardly at all.

The theoretical expression for the coupling strip was obtained by employing small obstacle theory, so that the result becomes less accurate as δ/a increases beyond its range of validity. Expression (32) may be valid up to $\delta/a = 0.25$ or so. In a practical configuration, δ/a may of course be made larger than that value if one wishes to obtain greater leakage per unit length, even though our theory becomes inaccurate in that range. By comparison with similar discontinuities, however, for which there are available both small obstacle results and ones for arbitrary dimensions, one can conclude that the small obstacle results, if extrapolated beyong their range of validity, yield values of coupling which are lower than the correct values. This means that the actual α/k values for large δ/a ratios are expected to be greater than the values computed using the small obstacle theory in the range beyond its validity.

As indicated above, the value of c/a must be selected in accordance with the optimization specified in Figs. 12. The ways in which β/k and α/k vary with c/a appear in Fig. 15(a) and (b). It is seen that β/k varies very little with c/a, whereas α/k is sensitive to it, with nulls appearing at those values of c/a for which the coupling strip is shorted out.

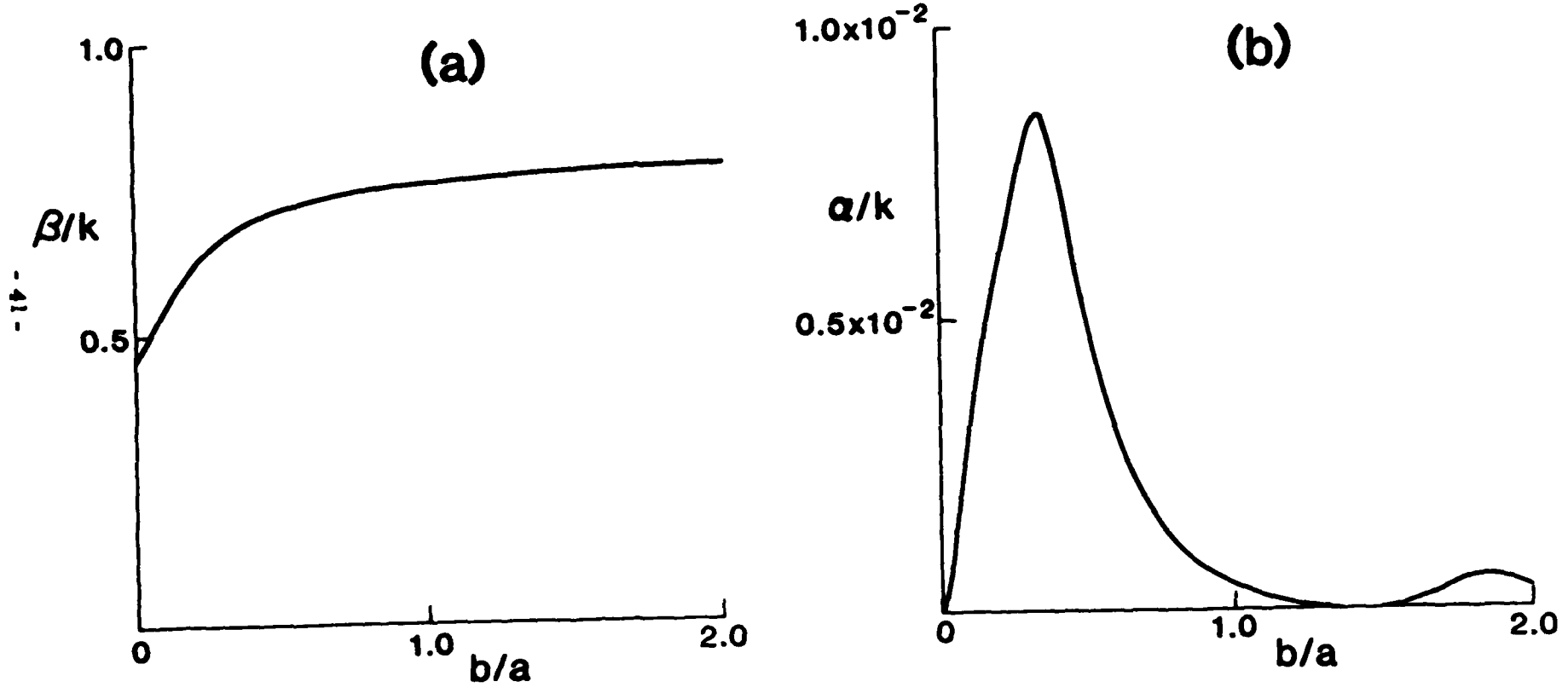

Fig. 13 The variations of β/k and α/k with the normalized groove guide height b/a, where the values of λ/a and the other dimensions are given in the box.

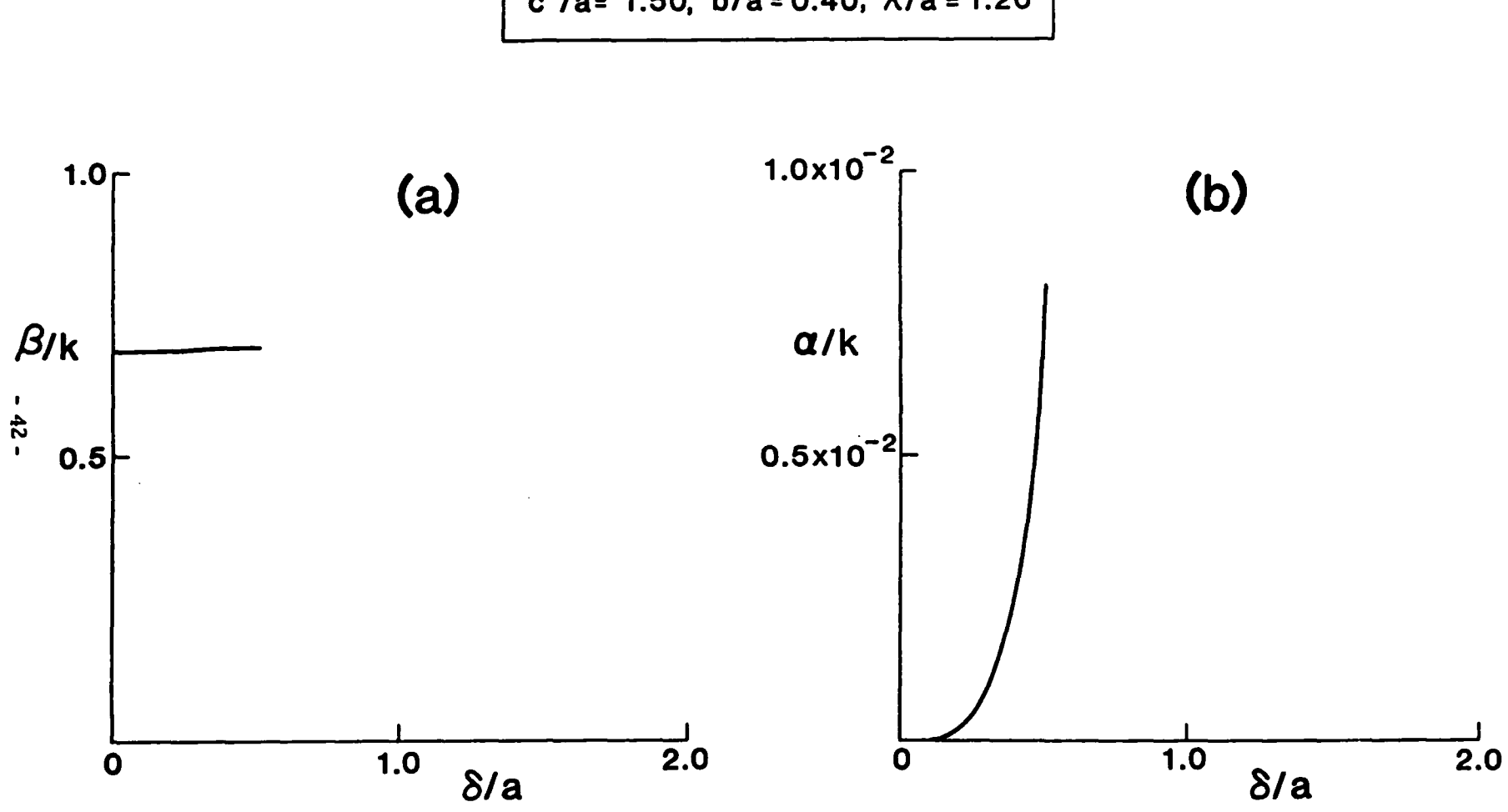

Fig. 14 The variations of β/k and α/k with the normalized length δ/a of the perturbing asymmetric strip; the values of λ/a and the other dimensions are given in the box.

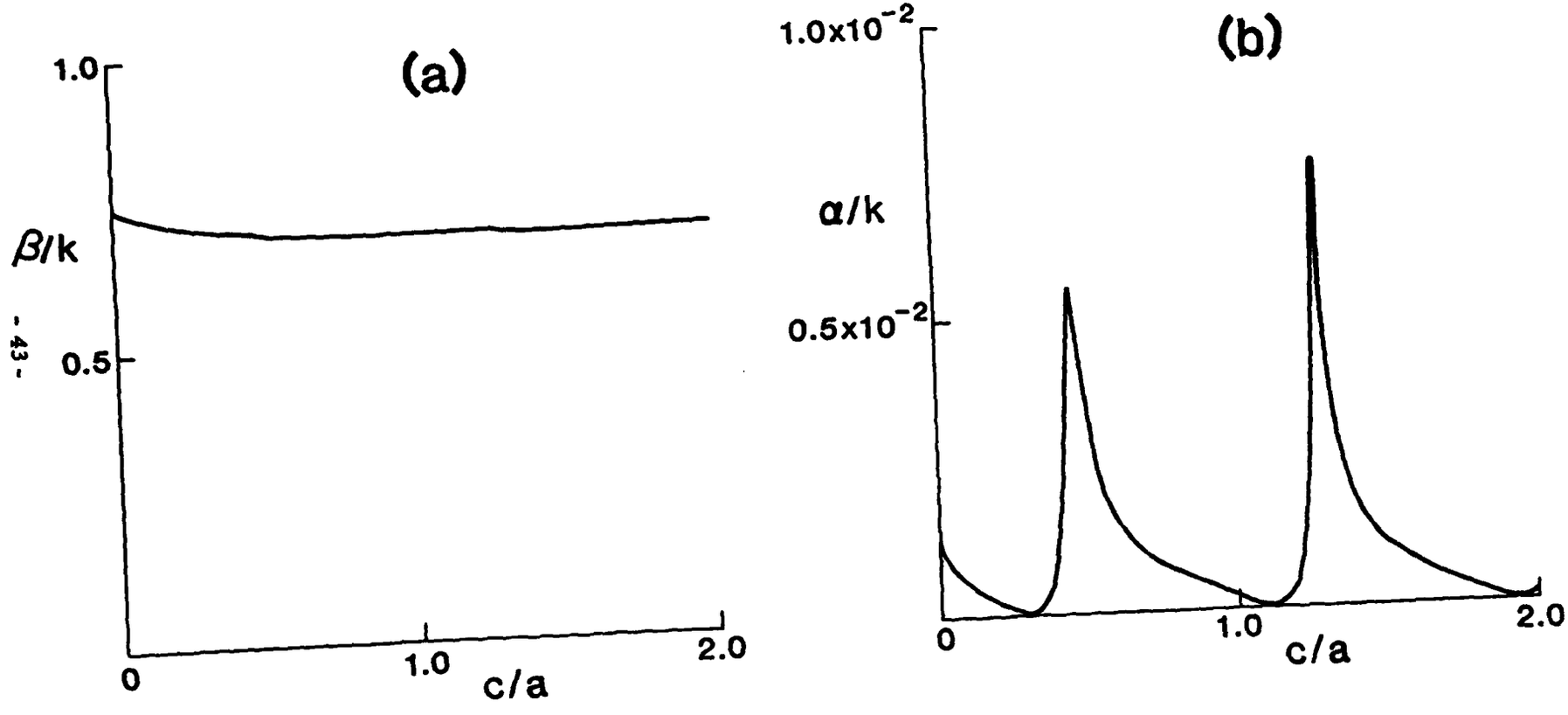

Fig. 15 The variations of β/k and α/k with the normalized length of guide c/a; the values of λ/a and the other dimensions are given in the box.

The final variations that we consider are those of β/k and α/k with c"/a, the normalized length between the coupling strip and the upper open end. Those variations are seen in Fig. 16(a) and (b). Because a standing wave in the i=0 transverse mode also exists in that length, we find that α/k varies with c"/a, so that it is necessary to select the best value of c"/a to optimize the value of α/k. We chose the peak at c"/a = 1.50 even though it results in a taller structure because we found that the field of the evanescent i=1 transverse mode had not yet decayed to negligible values at the c"/a value corresponding to the first peak.

The actual proportions in the cross section of the groove guide antenna corresponding to the optimizations discussed above are shown in Fig. 17. The antenna cross section ends up being tall and thin to insure that the i=1 transverse mode, which is evanescent in the regions of width a', has negligible amplitude at the very top and bottom.

In an actual antenna design, the value of α must be tapered, as indicated in Section E,1, but the value of β must remain essentially constant along the antenna length. From the curves in Figs. 13 through 16, we see that lengths c and c" are suitable parameters to vary for that purpose.

For the specific case corresponding to Fig. 17, the angle θ_m of the maximum of the radiated beam (see Fig. 9 and Eq. (48)) is about 44°, the length L of the antenna is about 25 free space wavelengths, in accordance with the conditions of Eq. (50), and the beam width is about 3.2°, from Eq. (49). It should be recognized that the optimizations discussed above are intended to increase the value of α/k, and thus to increase the beam width. It is easy to achieve a narrower beam, by simply relaxing the optimizations.

We have described here a new type of leaky wave antenna suitable for millimeter waves. It is based on the groove guide, which is a low-loss waveguide, so that the waveguide attenuation will interfere negligibly with the leakage process. The structure is simple and longitudinally continuous, rendering it reasonable for fabrication at the small wavelengths in the millimeter-wave range.

We have also derived all the constituents of an accurate transverse equivalent network, which yields a transverse resonance relation in closed form, from which numerical design values can be readily obtained.

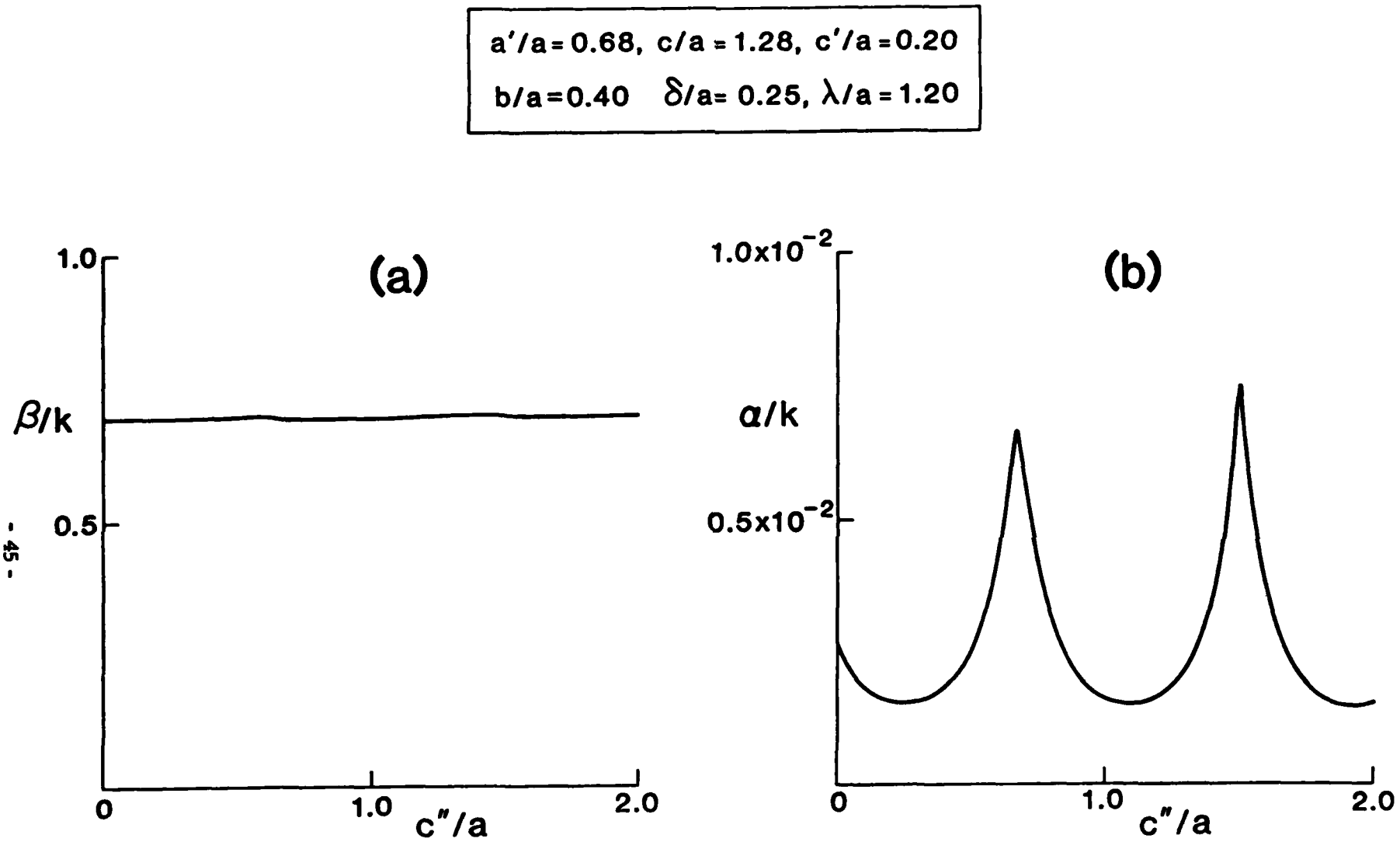

Fig. 16 The variations of β/k and α/k with the normalized length c''/a between the asymmetric strip and the upper open end; the values of λ/a and the other dimensions are given in the box.

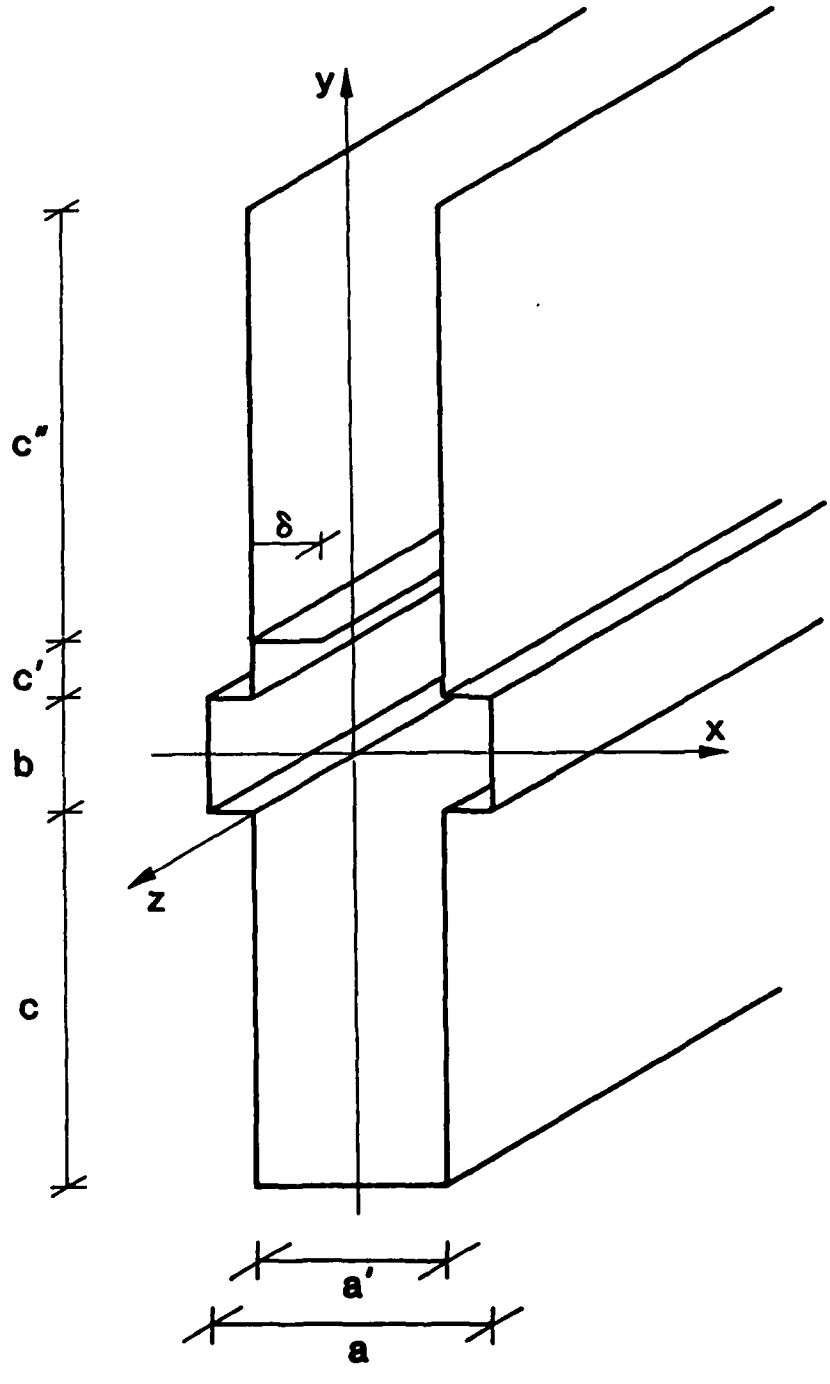

Fig. 17 The actual proportions in the cross section of the groove guide leaky wave antenna corresponding to the optimizations given in Figs. 12 through 16, and discussed in the text.

The antenna structure is therefore capable of straightforward understanding and systematic design. It is also sufficiently flexible with respect to the dimensional parameters which can be varied that a reasonably wide range of pointing angles and beam widths can be achieved with it.

REFERENCES

[1] T. Nakahara, Polytechnic Institute of Brooklyn, Microwave Research Institute, Monthly Performance Summary, Report PIBMRI-875, pp. 17-61, 1961.

[2] T. Nakahara and N. Kurauchi, "Transmission Modes in the Grooved Guide,", J. Inst. of Electronics and Commun. Engrs. of Japan, Vol. 47, No. 7, pp. 43-51, July 1964. T. Nakahara and N. Kurauchi, "Transmission Modes in the Grooved Guide," Sumitomo Electric Technical Review, No. 5, pp. 65-71, January 1965.

[3] H. Shigesawa and K. Takiyama, "Transmission Characteristics of the Closed Grooved Guide," J. Inst. of Electronics and Commun. Engrs. of Japan, Vol. 50, No. 11, pp. 127-135, November 1967. H. Shigesawa and K. Takiyama, "On the Study of a Closed Grooved Guide," Science and Engineering Review of Doshisha University, Japan, Vol. 9, No. 1, pp. 9-40, May 1968.

[4] F. J. Tischer, "The Groove Guide, a Low-Loss Waveguide for Millimeter Waves," IEEE Trans. on Microwave Theory Tech. vol. MTT-11, pp. 291-296, September 1963.

[5] J. W. E. Griemsmann, "Groove Guide," Proc. Symposium on Quasi-Optics, Polytechnic Press of Polytechnic Institute of Brooklyn, pp. 565-578, 1964.

[6] N. Y. Yee and N. F. Audeh, "Wave Propagation in Groove Guides," Proc. National Electronics Conf., Vol. 21, pp. 18-23, 1965.

[7] D. J. Harris and K. W. Lee, "Groove Guide as a Low-Loss Transmission System for Short Millimetric Waves," Electron. Lett., Vol. 13, No. 25, pp. 775-776, December 8, 1977. Professor Harris and his colleagues have published many papers on this topic, of which this is one of the first. One of their later works in given in Reference 8.

[8] D. J. Harris and S. Mak, "Groove-Guide Microwave Detector for 100 GHz Operation," Electron. Lett., Vol. 17, No. 15, pp. 516-517, July 23, 1981.

[9] J. Meissner, "Calculation of Coupling of Two Grooves in a Parallel-Plate Guide," Electron. Lett., Vol. 22, pp. 956-958, 1982.

[10] J. Meissner, "Radiation Losses of E-Plane Groove-Guide Bends," Electron. Lett., Vol. 19, pp. 527-528, July 1983.

[11] A. A. Oliner and P. Lampariello, "A Novel Leaky-Wave Antenna for Millimetre Waves Based on the Groove Guide," Electronics Letters, Vol. 18, No. 25/26, pp. 1105-1106, December 9, 1982.

[12] P. Lampariello and A. A. Oliner, "Theory and Design Considerations for a New Millimetre-Wave Leaky Groove Guide Antenna," Electronics Letters, Vol. 19, No. 1, pp. 18-20, January 6, 1983.

[13] H. M. Altschuler and L. O. Goldstone, "On Network Representations of Certain Obstacles in Waveguide Regions," IRE Trans. Microwave Theory Tech., Vol. MTT-7, pp. 213-221, April 1959.

[14] A. A. Oliner, "Equivalent Circuits for Slots in Rectangular Waveguide," Report R-234, Microwave Research Institute, Polytechnic Institute of Brooklyn, for the Air Force Cambridge Research Center, under Contract AF-19(122)-3, August 1951. This comprehensive report also contained contributions by J. Blass, L. B. Felsen, H. Kurss and N. Marcuvitz.

[15] A. A. Oliner and P. Lampariello, "Simple and Accurate Expression for the Dominant Mode Properties of Open Groove Guide," Digest of IEEE International Microwave Symposium, San Francisco, California, May 30-June 1, 1984.

[16] N. Marcuvitz, The Waveguide Handbook, Vol. 10, Radiation Laboratory Series, McGraw-Hill Book Co., New York, 1951.

[17] L. B. Felsen and W. K. Kahn, "Network Properties of Discontinuities in Multi-Mode Circular Waveguide," Proc. IEE (London), Part C, Monograph 503E, pp. 1-13, February 1962.

[18] F. Bardati and P. Lampariello, "The Modal Spectrum of a Lossy Ferrimagnetic Slab," IEEE Trans. Microwave Theory Tech., Vol. MTT-27, pp. 679-688, July 1979.

[19] See, for example, A. I. Markushevich, Theory of Functions of a Complex Variable, Vol. 2, Chapter 3, p. 109, Prentice-Hall Inc., Englewood Cliffs, New Jersey, 1965.

[20] P. Lampariello and R. Sorrentino, "The ZEPLS Program for Solving Characteristic Equations of Electromagnetic Structures," IEEE Trans. Microwave Theory Tech., Vol. MTT-23, pp. 457-458, May 1975.

MISSION
of
Rome Air Development Center

RADC plans and executes research, development, test and selected acquisition programs in support of Command, Control Communications and Intelligence (C^3I) activities. Technical and engineering support within areas of technical competence is provided to ESD Program Offices (POs) and other ESD elements. The principal technical mission areas are communications, electromagnetic guidance and control, surveillance of ground and aerospace objects, intelligence data collection and handling, information system technology, ionospheric propagation, solid state sciences, microwave physics and electronic reliability, maintainability and compatibility.

Printed by
United States Air Force
Hanscom AFB, Mass. 01731